The Precambrian Drift History and Paleogeography of India

Joseph G. Meert[1], Anthony F. Pivarunas[1], Scott R. Miller[1], Rachel F. Nutter[1],
Manoj K. Pandit[2], Anup K. Sinha[3]

[1]University of Florida, Department of Geological Sciences, 241 Williamson Hall, Gainesville, FL 32611
[2]Department of Geology, University of Rajasthan, Jaipur, Rajasthan India
[3]Dr. K.S. Krishnan Geomagnetic Research Laboratory, Chamanganj Bazaar, Allahabad 221 505, India

Feb 18, 2020

Abstract

We have compiled eleven reliable paleomagnetic poles from Peninsular India in order to test a variety of paleogeographic scenarios. Precambrian peninsular India represents an amalgam of five cratonic nuclei known as the Dharwar, Bastar, Singhbhum, Bundelkhand cratons and the Aravalli-Banded Gneiss Complex. The Bundelkhand craton and Aravalli-BGC (North Indian Blocks) are separated from the other three regions (South Indian Blocks) by an WSW-ENE trans-continental belt known as the Central Indian Tectonic Zone. Paleomagnetic and geochronological data from these regions indicate that the south Indian blocks were assembled by at least 1.765 Ga. Peninsular India was amalgamated along the CITZ between 1.1-0.9 Ga.

A picture of Peninsular India's nuclei is evaluated at discrete intervals and provides limited constraints on India's location in the Columbia and Rodinia supercontinents. The most robust paleogeographic pictures are at 1.88 Ga and at 1.45 Ga. We note several problems with the position of India in some existing maps of Rodinia between 1.1-1.0 Ga and argue that the 'tradition' of keeping East Gondwana intact for most of the Proterozoic is problematic. Lastly, we note that India contains a wealth of untapped 'paleogeographic resources' that promise to provide an improved picture of India's place in Precambrian supercontinents in the coming years.

Keywords: India, cratons, Rodinia, Columbia, supercontinent

Introduction

Precambrian peninsular India comprises five major lithotectonic units (Fig. 1) that were welded together either during the late Meso- to early Neoproterozoic (Fig. 1; 1200-1000 Ma; Meert et al., 2010; Bhowmik et al., 2012a, 2012b; Meert and Pandit, 2015;Bhowmik, 2019) or during the early Mesoproterozoic (~1.6 Ga; Naganjaneyulu and Santosh, 2010). These five units can be further subdivided into Northern Indian Block (NIB) that include the Bundelkhand Craton and the Aravalli-Banded Gneiss Complex (Fig. 1) and the Southern Indian Block (SIB) regions known as the Dharwar, Bastar and Singhbhum cratons (Fig 1). The NIB and SIB are separated by the WSW-ENE-trending Central Indian Tectonic Zone (CITZ; Fig. 1) that experienced polyphase metamorphism/deformation along its length (Stein et al. 2006, 2014; Meert and Pandit, 2015; Bhowmik, 2019). At the southern end of India lies the high-grade polymetamorphic terrane known as the Southern Granulite Province.

India has a long history of Precambrian paleomagnetic studies beginning with the pioneering work of Athavale et al. (1963) on the Malani Rhyolites (NIB), Gwalior Traps (Bundelkhand), Bijawar and Cuddapah Traps (Dharwar), followed by a study of the Upper Vindhyan sedimentary sequence (Bundelkhand; Sahasrabudhe and Mishra, 1966). Although paleomagnetic studies continued apace within Peninsular India, most of them lack detailed field tests (baked contact, fold, conglomerate) and reliable age control that limit their usefulness in continental reconstructions. Over the past two decades, paleomagnetic data from India significantly improved in average Q-value (Van der Voo, 1990; Fig. 2). In this review, we detail the criteria used to establish the most reliable poles for Peninsular India and use these poles to test a variety of proposed reconstructions of Columbia (aka Nuna; Hoffman, 1997; Rogers and Santosh, 2002; Meert, 2002;) and Rodinia (McMenamin and McMenamin, 1989; Li et al., 2008). At present, there are only eleven reliable poles from India and six poles predate the purported formation of the Paleo-Mesoproterozoic supercontinent Columbia (Nuna). Nevertheless, the paleomagnetic data from India have proven useful in detailing the growth and unification of Peninsular India and potential links in the aforementioned supercontinents at discrete intervals.

Data Selection

All previously published paleomagnetic poles from India were compiled and tabulated by the current authors as well as by the Precambrian working group at the most recent Nordic paleomagnetic workshop in Leirubakki, Iceland (2017; Brown et al., 2018). Paleomagnetic poles are searchable on the Paleomagia website (Veikkolainen et al, 2014). Each pole in this study was evaluated according to the criteria set forth in Van der Voo (1990). The Leirubakki working group used a 'modified' Q-value that eliminated the 7^{th} criteria (no resemblance to younger paleopoles). We use the original Q-criteria in our analysis (Q=7 max). In this compilation, we use only the poles that meet the following criteria: (a) poles must receive a $Q \geq 4$ (Van der Voo, 1990); (b) poles must have radiometric ages with errors of less than ±15 Ma; (b) and; (c) must show evidence that secular variation has been adequately averaged (McFadden et al., 1991; McElhinny and McFadden, 1997; Deenan et al., 2011). This reduced the total number of paleomagnetic poles used in this study to a total of eleven. All poles used in this study are calculated using a mean of virtual geomagnetic poles (VGP's) from one or more studies. In the following discussion, we provide a brief description of each cratonic region in India (Dharwar Craton, Fig. 3; Bastar Craton, Fig. 4; Singhbhum Craton, Fig. 5 and Bundelkhand Craton, Fig. 6) along with summaries of paleomagnetic data from that block.

Southern Indian Block (Dharwar, Bastar and Singhbhum cratons)

Dharwar Craton Results

The Dharwar Craton (Fig. 3) is the largest of the Indian nuclei, floored by Archean granites, greenstones and supracrustal rocks. Recent studies indicate its southern extent includes regions commonly lumped into the "Southern Granulite Terrane" (Pivarunas et al., 2019). The Dharwar craton is bounded to the northwest by the Deccan Traps, to the north by the Bastar Craton, to the east by the Eastern Ghats Mobile Belt, to the south by the Southern Granulite terrane and to the west by the Arabian Sea (Balakrishnan et al., 1999; Figs. 1 and 3).

Intrusive events in the Eastern Dharwar Craton (EDC) include generations of mafic dykes, kimberlites, and lamproites. Many of the clusters occur around the Cuddapah Basin and have three main trends: NW-SE, E-W, and NE-SW (Fig. 3; Samal et al., 2015). Söderlund et al. (2019) refer to these dykes by age/regional location. From oldest to youngest these swarms include (a) 2.37 Ga Banglarore-Karimnagar NE–SW to ESE–WNW trending swarm; (b) 2.25 Ga Ippaguda-Dhiburahalli N–S to NNE–SSW trending swarm; (c) 2.22 Ga Kandlamadugu N–S to NNW–SSE trending swarm; (d) 2.21 Ga Anantapur-Kunigal NW–SE to WNW–ESE trending swarm; (e) 2.18 Ga Mahbubnagar-Dandeli NW–SE to WNW–ESE trending swarm; (f) 2.08 Ga Debarabanda N–S, NW–SE and ENE–WSW trending swarm; (g) 1.88-1.89 Ga Hampi E–W to NW–SE trending swarm; (h) 1.788 Ga Pebbair NW–SE trending swarm. In addition to those described by Söderlund et al. (2019), there is a smaller suite of N-S trending alkaline dykes near Harohalli that are dated to 1.2 Ga (Pradhan et al., 2008).

Kimberlites and lamproites are found concentrated in four areas within the EDC bordering the Cuddapah Basin (Kumar et al., 2007; Fig. 3). They are characteristically potassic volcanic rocks that are occasionally diamondiferous. Robust age constraints were provided for many of these fields (Kumar et al., 2001; Kumar et al., 2007; Gopalan and Kumar, 2008) which suggest that the kimberlitic intrusions into the Dharwar craton were emplaced within the narrow time frame between ~1050-1130 Ma.

A total of 93 sites (791 samples; Table 1) were collected from the 2367 Ma E-W trending dykes that span much of the Dharwar Craton and the northern segment of the SGT (Fig. 3; Dawson and Hargraves, 1994, Radhakrishna and Joseph,1996; Halls et al., 2007, Piispa et al., 2011; Kumar et al., 2012a; Dash et al., 2013; Radhakrishna et al., 2013b, Belica et al., 2014, Valet et al., 2014, Babu et al., 2018; Pivarunas et al., 2019). A grand mean pole from these studies falls at 12.8° N, 62° E (A95=4.6°; Fig. 7a). The pole receives a Q=6 (did not meet criterion 7); however, the multiple positive baked contact tests significantly reduce the suspicion of remagnetization and we consider this a reliable pole for India at 2367 Ma.

Numerous dykes ranging in age from ~2207 to 2250 Ma have reported geochronologic and paleomagnetic results (Fig. 7b,c,d; Piispa et al., 2011; Kumar et al., 2012a,b, 2014, 2015; Radhakrishna et al., 2013b; Belica et al., 2014; Nagaraju et al., 2018a,b). Nagaraju et al. (2018a) reported a paleomagnetic pole from 2252 Ma dykes in the Dharwar Craton at 16° N, 119° E (α_{95}=9°) from a total of 9 dykes (64 samples; Table 1; Fig. 7b; see also Kumar et al., 2012a ;Belica et al., 2014;). We note that Nagaraju et al. (2018a) calculated a mean declination/inclination from widely separated dykes which was then used to calculate a paleomagnetic pole using a mean site located in the Bastar Craton (21° N, 77.9° E). This produces a slightly different pole from our mean (based on the average of VGP's; Table 1) for the 2252 Ma results at 12.8° N, 116° E (A95=14.2°). The pole receives a Q=4 and lacks any field tests; however, Nagaraju et al. (2018a) argue that the pole carries a primary magnetization on the basis of directional data from older and younger dykes with positive field tests.

Nagaraju et al. (2018b) compiled new and existing geochronological data on a long (450 km) north-south trending dyke known as the Andhra-Karnataka Long Dyke (AKLD; see also Srivastava et al., 2011; Kumar et al., 2014). The weighted mean age for this dyke is 2216 ± 0.9 Ma. A total of 21 sites (156 samples) were used to calculate a mean pole using the same methodology noted above (site location in Bastar craton) at 36° N, 132° E (a95=6°). Of the 21 sites, 17 were from various locations along the AKLD and the other 4 were compiled from previous publications (Piispa et al., 2011;Kumar et al., 2012a,b; Belica et al., 2014). Our calculation (Table 1) resulted in a mean pole at 33.5° N, 124° E (A95=6.6°; Fig. 7c). The pole receives a Q=5 (lacks field test and fails Q7 resemblance to younger paleomagnetic poles). The magnetization is older than 1885 Ma because dykes of that age cross-cut AKLD (Nagaraju et al., 2018b). Nagaraju et al. (2018a) argue that a positive reversals test with a rating of "C" is sufficient to argue for a primary magnetization (McFadden and McElhinny, 1990). Due to the fact that there are only 2 sites of opposite polarity, we used the simulation outlined by McFadden and McElhinny (1990) with an 'indeterminate' result. Heslop and Roberts (2018) proposed an alternative reversals test and the 2216 Ma pole receives a 'positive result' using that test. Radhakrishna et al (2013b) computed a mean direction for dykes they assigned to an age of 2215 ± 5 Ma that is significantly displaced from the mean pole calculated by Nagaraju et al. (2018b). The mean pole from Radhakrishna et al. (2013b) falls at 42° N, 186° E (A95=5°). Radhakrishna et al. (2013b) question the primary nature of 2216 pole calculated by Nagaraju et al. (2018b), based on the fact it is nearly identical to the pole from N-S oriented dykes in the Bastar Craton dated at 1465 Ma and the lack of a baked contact test. In this paper, we rely on the geochronological data provided by Nagaraju et al. (2018b), and cautiously use the 2216 Ma pole in our discussion.

Nagaraju et al. (2018a) compiled new and existing results from E-W and NW-SE trending dykes in the Dharwar Craton dated to 2206.8 ± 2.1 Ma. More recent geochronology shows a broader range in age for these dykes between 2200-2210 Ma (mean age 2207 Ma; Söderlund et al., 2019). The mean pole for the 2207 Ma swarm, calculated by Nagaraju et al. (2018a), falls at 57° N, 113° E (α_{95}=6°). We recalculated the pole based on the mean of VGP's for the widely distributed sites at 51.2° N, 108° E (Fig. 7d; A95=9.2°).

Published geochronological data from the 2.08 Ga Deverabanda dyke swarm (Kumar et al., 2015; Söderlund et al., 2019) show a narrow age range between 2081-2087 Ma for these N-S and NW-SE trending dykes. Kumar et al. (2015) combined paleomagnetic results from the studies by Piispa et al. (2011), Radhakrishna et al. (2013b) and Belica et al. (2014), to calculate a 2082 Ma pole at 40.5° N, 184° (Fig. 7e: A95=4.5°). The 2082 Ma pole is constrained by positive baked contact and reversal tests from 33 sites and 383 samples, and receives a Q=6 (Van der Voo, 1990).

A large swathe of E-W trending dykes ages between 1885-1894 Ma intrude the Dharwar Craton including sills within the lower Cuddapah sedimentary sequence in eastern Dharwar (Halls et al., 2007; French et al., 2008; Belica et al., 2014; Nagaraju et al., 2018b). These dykes also have age-equivalent NW-SE trending dykes in the Bastar Craton to the north (French et al., 2008; Meert et al., 2010;). In the Dharwar Craton, these dykes are known as the Hampi Swarm (Söderlund et al., 2019). The ~1888 Ma paleomagnetic pole, calculated from dykes in both the Dharwar and Bastar cratons, falls at 35° N, 334° E (Fig. 8a, A95=4.6°) and is based on studies of 54 sites (434 samples). The pole receives a Q=7 (Van der Voo, 1990).

Bastar Craton

The Bastar (sometimes referred to as the Bhandara or Central Indian) Craton is bordered by the Godavari Rift (to the south); by the Mahanadi Rift (to the northeast); by the Central Indian Tectonic Zone (to the north); by the Eastern Ghats Mobile Belt (to the east) and the Deccan Traps (to the west; Figs. 1 and 4). Two main basement assemblages form the core of the craton and are known as the "Gneissic Complex". The gneisses are intruded by a younger suite of granitic plutons and mafic dykes. Sparse radiometric data are reported from the Bastar Craton. The basement "Gneissic Complex" contains tonalite-trondhjemite gneisses and granites with ages between 2.5-2.6 Ga (Sarkar et al., 1981; Sarkar et al., 1990; Sarkar et al., 1993; Santosh et al., 2004; Ramakrishnan and Vaidyanadhan, 2008). Older ages are reported from the basement rocks of ~3.6 Ga (; Sarkar et al., 1993; Ghosh, 2004; Rajesh et al., 2009). Granitoid bodies range in age from 2.1-3.0 Ga (; Bandopadhyay et al., 1990; Sarkar et al., 1990, 1993, 1994). The Bastar Craton contains two large sedimentary basins, the Chhattisgarh Basin and the Indravati Basin along with four minor basins with poorer age constraints (Meert and Pandit, 2015; Fig. 4). It is likely that these were all part of a single large basin and the outcrops are now isolated via differential erosion. Like many of the Purana basins in India, the chronological history of the Chhattisgarh Basin is controversial.

The Bastar Craton is intruded by numerous mafic dyke swarms that cross-cut the basement (French et al., 2008). The majority of the dykes in the southern Bastar Craton trend NW-SE, paralleling the Godavari Rift. The northern Bastar dykes trend NNW-SSE and are oblique to the Mahanadi Rift (French et al., 2008; Fig. 4). Limited geochronological controls exist for the dykes in the Bastar Craton, although the NW-SE swarm yielded two reliable U-Pb ages of 1891 ± 0.1 Ma and 1883 ± 1.4 Ma (French et al., 2008). A second suite of mostly N-S trending dykes (southeast of Raipur; Fig. 4) of more variable geochemistry yielded overlapping ages including a SHRIMP U-Pb age of 1444 ± 30 Ma (Ratre et al., 2010) and a U-Pb zircon age of 1466 ± 2.6 Ma for a rhyolitic dyke (Pisarevsky et al., 2013). More recently, a suite of bonititic dykes (NW-SE trending; southern Bastar Craton) were dated to 2365.6 ± 0.9 Ma (Liao et al., 2019).

Two paleomagnetic studies from the Bastar Craton offer reliable poles that are used in this study. The first study is from the 1.88 Ga dykes that are coeval with the Hampi Swarm (Dharwar Craton, see previous section and Fig. 8a). The results from these dykes (Meert et al., 2010; Radhakrishna et al., 2013a) were combined with those in the Dharwar Craton (see previous section). The second paleomagnetic pole is from the ~1465 Ma Lakhna dykes (Pisarevsky et al., 2013). The Lakhna dykes produced a mean pole at 35.7° N, 132° E (Fig. 8c; A95=15.5°) and receive a Q=6 (Van der Voo, 1990; lack a field test).

Singhbhum Craton

The 40,000 km^2 Singhbhum Craton is the most northerly of the South Indian Block nuclei (Figs. 1 & 5). It comprises four major units: Older Metamorphic Group (OMG), Older Metamorphic Tonalite Gneisses (OMTG), Iron Ore Group (IOG), and Singhbhum Granite Complex (Miller et al., 2018, and references therein). The metasedimentary rocks and amphibolites of the OMG and tonalite-trondhjemite gneisses of the OMTG occur as small enclaves within the Singhbhum Granite, which makes up the dominant portion of the Singhbhum Craton nucleus. The Iron Ore Group is arranged in three volcano-sedimentary basins surrounding the east, south, and west sides of the Singhbhum Granite Complex. Secondary units such as the Dhanjori Volcanic rocks, Simlipal Basin, and Dalma Volcanic rocks were added to the craton from Neoarchean to Proterozoic time (Fig. 5; Mahadevan, 2002; Misra and Johnson, 2005; Bhattacharya et al., 2015).

The Archean lithologies – particularly the Singhbhum Granite (Fig. 5) are cut by a dense array of dykes known as the 'Newer Dolerites'. The Newer Dolerites fall into *at least* 4 pulses with well-determined ages: 2800 Ma, 2762 Ma (Kumar et al., 2017), 2260 Ma (Srivastava et al., 2019), and 1765 Ma (Shankar et al., 2017). Until these recent data, geochronological control on the emplacement ages for the Newer Dolerites was poor, with the K-Ar system yielding (roughly grouped) ages ranging between 2200-900 Ma (Naqvi and Rogers, 1987; Srivastava et al, 2000; Mukhopadhyay, 2001; Bose, 2008). Srivastava et al. (2019) separate the Newer Dolerites into as many as 7 swarms, with the latest dyke activity occurring post-1765 Ma.

Only a few paleomagnetic data exist for the Singhbhum Craton. Results from the Neoarchean dykes (~2763 Ma) of Singhbhum craton lack evidence for a primary remanence (Kumar et al., 2017). Preliminary work by Pivarunas et al. (2018) indicates a widespread younger overprint throughout the Singhbhum Craton, yielding steep directional data identical to that of the 2763 Ma dykes. Shankar et al. (2017) published paleomagnetic results on a suite of NNW-SSE trending dykes that were previously dated to 1765 Ma based on Pb-Pb ages on baddeleyite (Shankar et al., 2014). A total of 9 sites (86 samples) yielded a paleomagnetic pole at 44.9 N, 311

E (Fig. 8b; A95=8.7). The pole is graded Q=6 (lacks reversals) and is the only key pole from the Singhbhum craton.

Northern Indian Block (*Aravalli-Delhi-Marwar-Banded Gneiss Complex/Bundelkhand Craton*)

Figures 1 and 6a,b show the region of India that is positioned to the north of the Central Indian Tectonic Zone (CITZ). The Aravalli Banded Gneiss Complex is separated from the Bundelkhand-Gwalior region by the Great Boundary Fault. Bhowmik et al. (2012a) synthesized the available geochronological data into a plate-tectonic framework for the development of the BGC region. The 3.3 Ga granite gneisses represent the basement while ~2.5 Ga granitic intrusions mark stabilization of the craton (Sinha-Roy et al., 1998; Roy and Jakhar, 2002). The Aravalli Supergroup sedimentary rocks were deposited between 2.4-2.1 Ga (, Deb, 1999; Deb and Thorpe, 2004); however, more recent detrital zircon studies favor much younger sedimentation ages (McKenzie et al., 2013; Wang et al., 2019). The Aravalli sequence was subsequently metamorphosed and deformed (Sinha Roy et al., 1998; Roy and Jakhar, 2002). Onset of sedimentation in the Delhi Basin also lacks precise control and the 'best' estimates for the opening and closure of the basin are 1.7 and 1.45 Ga respectively (Roy and Purohit, 2015). A widespread phase of deformation in the Delhi Fold Belt at ~1.0 Ga coincides with a major phase of deformation throughout India (Deb et al., 2001; Leelanandam et al., 2006; Meert et al., 2013; Vijaya-Rao and Krishna, 2013; Bhowmik, 2019) and cessation of sedimentation in several of the larger "Purana" basins (Gupta et al., 1997; McKenzie et al., 2001; Deb et al., 2001; Malone et al., 2008; Meert et al., 2013; Turner et al., 2014; Patranabis-Deb et al., 2007; Meert and Pandit, 2015). Following the compressional deformation in the early Neoproterozoic, widespread felsic-dominated volcanism is consistent with an active continental margin along NW India until ~750 Ma (Malani-Erinpura igneous rocks; Vijaya-Rao and Krishna, 2013) and finally deposition of the Neoproterozoic-Cambrian Marwar Supergroup sequence (Meert and Pandit, 2015 and references therein).

Paleomagnetic studies from the Northern India Block (NIB) and the western margin of the Aravalli-BGC region (Malani) are given in Table 1. Perhaps the most robust Neoproterozoic pole from Peninsular India (Q=7) is derived from multiple investigations of the Malani Igneous Province (Fig. 6a; Athavale et al., 1963; Klootwijk, 1975; Torsvik et al., 2001; Gregory et al., 2009; Meert et al., 2013). The Malani grand mean pole falls at 69.4° N, 75° E (Fig. 9b; A95=6.4°). The U-Pb age determinations from late stage mafic dykes along with rhyolitic flows constrain the age of this pole to between 750-771 Ma (Gregory et al., 2009; Meert et al., 2013; Wang et al., 2017).

Three different paleomagnetic studies (between 1050-1115 Ma) from intrusive rocks within the Bundelkhand Craton (Miller and Hargraves, 1994; Gregory et al., 2006; Pradhan et al., 2012; Radhakrishna et al., 2013a) along with multiple studies of the Upper Vindhyan sedimentary sequence (Fig. 6b; Athavale et al., 1972; Klootwijk, 1973; McElhinny et al., 1978; Malone et al., 2008) are used to calculate our mean 1075 Ma directions. The Majhgawan kimberlite (Fig. 6b; 1073.5 ± 14 Ma) virtual geomagnetic pole (VGP) falls at 37° N, 213° E (α_{95}=15.3°). Pradhan dated the ENE-WSW-trending Great Dyke of Mahoba (Fig. 6b) and satellite dykes to 1113 ±7 Ma with a VGP at 37.8° N, 229.5° E (α_{95}=15.5°). Radhakrishna et al. (2013a) reported directions from 4 dykes with shallow inclinations and correlated these with the Great Dyke of Mahoba. Directional data from those 4 dykes yielded a VGP at 47° N, 193° E (α_{95}=22°). The paleomagnetic pole from the Upper Vindhyan Supergroup (Bhander and Rewa groups) was obtained from the results of Klootwijk, 1973; McElhinny et al., 1978 and Malone et al, 2008. The grand mean Vindhyan pole is located at 48° N, 215° E (α_{95}=5.8°). The results of Sahasrabudhe and Mishra (1966) and Athavale et al. (1972) are omitted because they did not apply stepwise vector demagnetization to isolate a final direction. As noted above, the age of the Upper Vindhyan sequence is controversial. The onset of sedimentation must have occurred prior to 1073 Ma as the Majhgawan kimberlite intrudes the lowermost member (Kaimur Group) of the Upper Vindhyan. Malone et al. (2008) argued that much of the sedimentation in the Upper Vindhyan ended at ~1000 Ma due to the lack of any younger detrital zircons. Subsequent detrital zircon studies also lack zircon populations younger than 1000 Ma (McKenzie et al., 2011; Turner et al., 2014) and low-precision Pb-Pb carbonate ages also support this conclusion (Gopalan et al., 2013). Similar-age results from the Dharwar craton kimberlites (Venkateshwarlu et al., 2013) yield a virtual geomagnetic pole at 44.5° N, 195° E (α_{95}=15.2°). The mean pole calculated from the VGP's of 56 sites (500 samples) from the Upper Vindhyan, Majhgawan kimberlite, Mahoba dykes and Dharwar kimberlites falls at 44.4° N, 215° E (Fig. 9a; A95=3.3°). We assign an age of 1075 Ma for this pole (Q=5).

There are three Paleoproterozoic poles from dykes intruding the Bundelkhand craton (Pradhan et al., 2010, 2012; Radhakrishna et al., 2013a). Only one of the poles has a reliable U-Pb age of 1979 ± 8 Ma. A combined mean pole from the 1979 Ma dykes (22 sites/263 samples) falls at 57.5° N, 309° E (Fig. 7e; A95=4.8°; Pradhan et al., 2012; Radhakrishna et al., 2013a). The dual-polarity magnetization has a baked contact test (Pradhan et al., 2012) which demonstrates its primary nature and receives a Q=6 according to the Van der Voo (1990) criteria.

Orogenic Belts of Peninsular India

There are three main regions of Peninsular India that have experienced tectonothermal events. The Central Indian Tectonic Zone (or CITZ; Figure 1) is the locus of polyphase orogenic activity related to the collision of the NIB and SIB during the Meso-Neoproterozoic. Bhowmik (2019) provides a useful synthesis of the available geochronological, thermobarometric and deformational history within the CITZ. The CITZ records three phases of development beginning with the 1.6-1.5 Ga assembly of 'proto-India' via the accretion of arc-related terranes to the margins of the SIB during the consumption of the ocean separating the NIB/SIB. At around 1.4 Ga, proto-India disintegrates as extension occurs along the Satpura and Chottanagpur belts (Fig. 1). Although the extent of oceanic crust developed between the proto-Indian blocks at ~1.4 Ga is poorly known, structural, geochronological and thermobarometric data indicate a Himalayan-type collision between SIB, the NIB and the Marwar Block around 1.0 Ga. Geophysical data suggest that the SIB was thrust beneath the NIB at this time.

The Eastern Ghats Mobile Belt lies along the eastern margin of Peninsular India (EGMB; Fig. 1). Dasgupta et al. (2017) make the case for multiple phases of deformation in the EGMB related to the assembly and disaggregation of Columbia and Rodinia, followed by the formation of Gondwana. In their scenario, the EGMB forms the locus of accretion between the Dharwar and Bastar cratons and the Napier Complex of East Antarctica between 1.6-1.5 Ga. This interval overlaps with events in the CITZ as does the later rifting at 1.4 Ga. The ocean basin developed during Columbia rifting closed again between 1.03-0.99 Ga during the presumed assembly of Rodinia, perhaps with a larger portion of East Antarctica. Rifting takes place again at around 780 Ma and the regions are re-assembled between 550-500 Ma during final Gondwana formation. Meert et al. (2017) refer to this model as 'yo-yo' tectonics because the geometries proposed by Dasgupta et al. (2017) show little change in the relationship between the Napier Complex region of East Antarctica and the SIB during each phase of assembly and dispersal.

The Southern Granulite Terrane (SGT) is separated from the Dharwar craton along the Palghat-Cauvery Shear Zone (PCSZ) near the southern tip of Peninsular India (Fig. 1). The geology and evolution of the SGT is complex and beyond the scope of this paper; however, its

Neoproterozoic evolution is integral to understanding the assembly of Gondwana (Meert, 2003; Collins et al., 2014). The region likely represents an amalgam of terranes including pieces formerly part of Madagascar, Sri Lanka and East Antarctica that were ultimately assembled during the destruction of the Mozambique Ocean, culminating with the Kuunga Orogeny (~550-500 Ma) and formation of Gondwana.

Geomagnetic Field, Paleoclimate and Greater India Assembly

Each of the paleomagnetic poles used in this study were analyzed for paleosecular variation and reversal frequency (see Table 1). Although the data are limited in scope, each of the poles adequately averaged paleosecular variation based on the crtieria set forth in Deenen et al. (2011, 2014). The data were also compared to the Model-G fields of McElhinny and McFadden, 1997 (0-5 Ma); Veikkolainen and Pesonen, 2014 (1.0-2.2 Ga and 2.2-3.0 Ga) and Biggin et al., 2008 (0-195 Ma). Figure 10a shows each of the paleomagnetic poles along with their estimate of geomagnetic secular variation (S_B) and 95% confidence limits (Cox,1969). The data most closely follow the Model-G curve of Biggin et al. (2008) for the 0-195 Ma time interval, but the errors also overlap with the McElhinny and McFadden (1997) 0-5 Ma field model. The only outlier are the results from 1888 Ma dykes. The data deviate substantially from the Precambrian Model G fits proposed by Veikkolainen and Pesonen (2014).

A paleolatitudinal drift plot for India is shown in Figure 10b along with lithological indicators of paleoclimate. The use of Phanerozoic paleoclimatic indicators in the Precambrian is fraught with problems. The occurrence of at least 3 episodes of global glaciation (Hoffman and Schrag, 2002; Hoffman et al., 2017) negates the use of glacial deposits for latitudinal indicators. Only one potential glaciogenic deposit is identified in Peninsular India within the Sausar Group (Mohanty, 2015; Sarangi et al., 2017) at c. 2.4 Ga; however, Bhowmik (2019) questions the age constraints of these rocks. Other commonly used paleoclimatic indicators for Phanerozoic include carbonates, evaporites and coals (Scotese and Barrett, 1990). Carbonate rocks occur over a fairly wide-range of paleolatitudes; however, they are more frequent between 0º-35º. Phanerozoic evaporite deposits are dominant between the latitudes of 15º-40º. Coals are non-existent in the Precambrian. In addition to the lack of strong climatic indicators, the ages of sedimentary rocks within India are poorly constrained (see Meert and Pandit, 2015 and references therein). In order to extend our plot from 2.4 Ga to 541 Ma, we have included paleomagnetic data from the Marwar Supergroup (Davis et al., 2014), presumed Ediacaran-Cambrian overprints in the Dharwar craton (Halls et al., 2007; Pradhan et al., 2008; Belica et al., 2014; Pivarunas et al., 2019) that indicate low paleolatitudes. Latitudinal drift rates computed in this study range between 0.4-4.4 cm/yr. Alkaline dykes from the Harohalli region (Pradhan et al., 2008) may indicate slightly faster drift rates of ~7 cm/yr between 1.2-1.075 Ga (Figure 10b).

Although the paleomagnetic database from India is now far more extensive than at the turn of the century, some of the questions regarding the assembly process remain unanswered. We outline the current status based on paleomagnetic and geochronologic data. Srivastava et al. (2019) use only geochronological data in their analysis and conclude that the Singhbhum and Bastar cratons were fellow travelers by 2.7 Ga and that the Southern India blocks were assembled by 2.2 Ga (Fig. 10c). There are no (as yet) 2.2 Ga dykes from the Bastar Craton so we take a more conservative approach by combining paleomagnetic and geochronological data to evaluate India assembly.

In our analysis, the northern block of the Southern Granulite Terrane (SGT) and the Dharwar craton were part of the same block by 2.36 Ga as both paleomagnetic data and geochronology from those regions agree (Halls et al., 2007; Dash et al., 2013; Belica et al., 2014; Pivarunas et al, 2019). Recent geochronological data from NE Dharwar and Bastar cratons (Demirer, 2012; Kumar et al., 2012b; Liao et al., 2019) demonstrate that the 2.37 Ga swarm extends into the Bastar Craton linking the Dharwar, Bastar and northern Southern Granulite Terrane in the early Paleoproterozoic (Figs. 10c, 11a). This is confirmed by our own (unpublished paleomagnetic) observations from the 2.37 Ga bonititic dykes in the Bastar (Liao et al., 2019). The Bastar and Dharwar cratons also show identical ages and paleomagnetic directions for the suite of 1.88 Ga dykes (French et al., 2008; Meert et al., 2010; Belica et al., 2014). This strong agreement between the Bastar and Dharwar dykes indicates that models positing a later, ~1.6 Ga collision, between those two blocks resulted from intracratonic deformation rather than collision.

The inclusion of the Singhbhum craton into the southern Indian block is difficult to assess based on combined paleomagnetic and geochronological data. There is only one reliable pole from the Singhbhum Craton (Shankar et al., 2017) and no paleomagnetic poles of similar age from either the Bastar or Dharwar cratons. Therefore, we tentatively conclude that the SIB had assembled by *at least* 1765 Ma based on geochronological data alone (Fig. 10c, 11b; Shankar et al., 2014; Shankar et al., 2017; Kumar et al., 2017; Srivastava et al., 2019). Paleomagnetic and geochronological studies of 2.2 Ga dykes from the Singhbhum and Bastar cratons may provide an important test for earlier coalescence of the SIB.

Numerous ultramafic bodies intrude the Bundelkhand and Dharwar cratons with ages between 1050-1125 Ma (Figs. 3 & 6; Miller and Hargraves, 1996; Gregory et al., 2006; Pesonen et al, 2012; Sahu et al, 2013; Venkateshwarlu and Chalapathi Rao, 2013). Paleomagnetic data from the Majhgawan kimberlite (1073 Ma; Miller and Hargraves, 1996; Gregory et al., 2006), the Bhander-Rewa sedimentary rocks and the Mahoba dykes (1113 Ma; Pradhan et al., 2012; Radhakrishna et al., 2013a) of the Bundelkhand craton show good agreement with a with ~1100 Ma kimberlite rocks in the Dharwar craton (Venkateshwarlu and Chalapathi-Rao, 2013); however, other studies on kimberlites from the Wajrakarur field (~1100 Ma) indicate much steeper directions than those from Bundelkhand Craton (Miller and Hargraves, 1996; Pesonen et al., 2012). Although the paleomagnetic data are debatable, the Central Indian Tectonic Zone (CITZ) is dominated by 1100-900 Ma tectonothermal deformation and metamorphism that is consistent with our conjecture of final assembly of Peninsular India (Bhowmik, 2019; Fig 10c, 11c).

The scenario described above is based solely on our assessment of the extant paleomagnetic database. Bhowmik (2019 and references therein) provides a different view on the suturing of the NIB/SIB regions that is not inconsistent with the scenario outlined above. In his model, a 'proto-Greater India' forms between 1.62-1.57 Ga, but is not fully welded until ~1.0 Ga.

The growing geochronological database from Dharwar craton together with trends of (selected) dated dykes has been used to argue for an intracratonic rotation between north and south Dharwar Craton (Söderlund et al., 2019). The paleomagnetic results from the dated dykes in question - indeed from any dykes in Dharwar Craton - were not utilized as a test of intracratonic rotation. Preliminary investigation of the declination changes between the northern and southern segments of the Dharwar Craton provide some support for this proposal; however, the magnitude of the rotation is poorly resolved given the statistical limitations of steep directional data (i.e. from the 2367 Ma and 2250-2207 Ma dyke swarms). We do note that there is no evidence of systematic changes in declination from the 1885 Ma dykes from northern Dharwar/Bastar and southern Dharwar cratons suggesting that any rotations may have occurred prior to 1885 Ma.

India in a Global Context

The development of a coherent Proterozoic Apparent Polar Wander Path (APWP) for India is difficult given the gaps in paleomagnetic data along with the aforementioned complex assembly history. Figure 12 shows all the poles from Table 1. The data are dominated by pre-Columbia/Nuna poles between 2.0-2.4 Ga. The best-constrained segment of an apparent polar wander path is for the Dharwar Craton between 2.4-2.2 Ga. If the southern Indian blocks form a coherent assembly by ~1.9 Ga, then a path can be drawn from 1.9-1.47 Ga (Fig. 12) albeit with a 300 Ma gap between the 1.765 and 1.465 Ga poles. A similar age gap exists for the assembled Peninsular Indian blocks between 1.075-0.77 Ga (Fig 12). There are two disparate paleomagnetic poles from the Dharwar Craton at ~1.2 Ga that could potentially add to the database. The Harohalli alkaline dykes pole (25º N, 78º E; Pradhan et al., 2008) indicates very high paleolatitudes for the Dharwar craton (Fig. 10b). Unfortunately, the dated dyke in that study did not yield useful paleomagnetic results and so the relationship between the dated dyke and the dykes that provided paleomagnetic results is unclear. In addition, the study lacked any field tests for a primary magnetization. The second pole (50.1º N, 67.4º E) is derived from limestones and shales from the Prahnita-Godavari and Chhattisgarh basins (Fig. 1; de Kock et al., 2015). The paleomagnetic pole appears to be primary based on an intraformational conglomerate test and a regional fold test. Unfortunately, there are no good geochronologic data from the sedimentary sequences although they are bracketed to between 1.4-1.0 Ga (Meert and Pandit, 2015; Chakraborty et al., 2015).

India is included in both Columbia (Nuna) and Rodinia (Rogers and Santosh, 2002; Zhao et al., 2004; Li et al., 2008; Meert, 2012, 2014; Meert and Santosh, 2017). Most reconstructions place all of Peninsular India at a peripheral location in these supercontinents. Given the limited paleomagnetic data from India (and globally), our reconstructions are based on widely spaced paleomagnetic poles from India and elsewhere. We use a 'closest approach' methodology at discrete intervals to show possible locations of the Indian blocks with respect to other regions where similar-age poles exist. We note that neither longitude nor hemisphere are constrained by these data. The lack of a detailed apparent polar wander path for the Indian blocks creates difficulty linking an Indian APWP with better known APWP's from other continents.

2.367 Ga Schematic

The Dharwar-Bastar cratons are contiguous at 2367 Ma based on geochronological and paleomagnetic data. Halls et al. (2007) posited a possible connection between the 2410 Ma Widgiemooltha dykes of the Yilgarn craton (Australia; Evans, 1968; Smirnov et al., 2013) and Indian dykes as expressions of a long-lived plume in the Siderian Period (Fig. 13a). Belica et al. (2014) showed that link was implausible given the nearly 25° latitudinal difference between the two cratons as well as the short, 5 Ma, duration of dyke activity in the Dharwar Craton (Kumar et al., 2012a). Furthermore, a younger (2401 Ma) pole from the Yilgarn Craton (Pisarevsky et al., 2014) indicates a much greater latitudinal offset between the two regions. Only one other reliable pole from the Kaapvaal craton (Gumsley et al., 2017) is available for this time interval making further paleogeographic conjectures premature.

2.22 Ga Schematic

India has a rather well-constrained APWP segment between 2.252 Ga and 2.207 Ga (Table 1; Fig. 10b). Most of the motion of India is rotational during this time interval so we choose 2.22 Ga for our reconstruction. Paleomagnetic data of similar age are derived from the 2.216 Ga Senneterre and Nipissing regions of the Superior Craton (Buchan et al., 1993; Buchan et al., 2000), the 2.231 Ga Malley dykes of the Slave Craton (Buchan et al., 2012) and the 2.225 Hekpoort Formation within the Kaapvaal Craton (A-component, Humbert et al., 2017). Figure 13b shows the paleolatitudinal distribution of these blocks. The Slave and Superior provinces were still separated by the Manikewan Ocean at this time (Pehrsson et al., 2015). The Bastar and Dharwar cratons of southern India were located at intermediate latitudes.

2.08 Ga Schematic

Data for our 2.08 Ga schematic (Table 2; Fig. 13c) are derived from a mean pole calculated from the ~2079 Ma Lac Esprit, Cauchon Lake and Ft. Frances studies in the Superior Craton (Evans and Halls, 2010); the Bushveld Complex of the Kaapvaal Craton (Kaapvaal-B 2049 Ma;

Letts et al., 2007); The Waterberg-UBSI (Kaapvaal-A 2054 Ma; de Kock et al., 2006), Mean Guiana Shield pole (2093 Ma; Théveniaut et al., 2006); the Kangalmut dykes of Greenland (2042 Ma; Fahrig and Bridgewater, 1976) and the Kuetsyarvi Formation of Fennoscandia (2059 Ma; Torsvik and Meert, 1995). Close connections between Fennoscandia, Greenland and the Superior province are permissible.

1.88 Ga Schematic

Paleomagnetic data (Table 2) are more abundant at ~1.88 Ga and we use paleomagnetic poles from India; two options from the Amazonian, Slave, Superior and Kaapvaal cratons, and Fennoscandia as well as one pole from Siberia. This time interval marks the onset of Columbia/Nuna assembly (see also Pehrsson et al. 2015; Meert and Santosh, 2017); however, assembly of Laurentia is not yet completed (Killian et al., 2016; Fig. 14a).

1.77 Ga Schematic

The supercontinent of Columbia/Nuna is thought to be largely intact by 1.77 Ga (Meert and Santosh, 2017;); however, high quality paleomagnetic data are lacking from much of the globe. We compiled the most reliable paleomagnetic data from this interval which includes the 1765 Ma, NW-SE trending Newer Dolerite swarm (Table 2; Shankar et al., 2017); a ~1785 Ma pole from multiple studies in Fennoscandia and a 1755 Ma pole from Sarmatia; a 1789 Ma pole from Amazonia; 1780 Ma pole from the North China Block and a younger 1732 Ma pole from the Aldan Shield (Siberian craton). The available paleomagnetic data do not provide a strong picture of the assembled (or nearly so) Columbia/Nuna supercontinent, but geological evidence is strongly supportive of a large continental assembly (Meert and Santosh, 2017). We note that Killian et al. (2016) argue for a unified Laurentia (Slave, Superior, Wyoming, Greenland and intervening mobile belts) by ~1750 Ma. Meert and Pandit (2015) conclude that the southern Indian blocks coalesced no later than 1765 Ma. Bogdonova et al. (2016) conclude that much of Baltica was assembled by 1750 Ma as was Siberia (Gladkochub et al., 2008) and western, northern and southern Australia (Cawood and Korsch, 2008; Wingate and Evans, 2003).

Zhao et al. (2004) posited long-lived links between the North China Craton and India in the Columbia configuration. The argument was based on the supposed contiguity of 2.1-1.9 Ga mobile belts transiting the North China Craton (Trans North China Orogen or TNCO) and the Central Indian Tectonic Zone (CITZ). There is little, or no evidence, for significant tectono-thermal activity in the CITZ during the 2.1-1.9 Ga interval (see Bhowmik, 2019). Nevertheless, paleomagnetic data from India and the North China Craton at ~1765 Ma and ~1465 Ma (see below) are compatible with the paleogeography proposed by Zhao et al. (2004).

1.45 Ga Schematic

Figure 14c shows a reconstruction at 1.45 Ga that follows the analysis provided in Meert and Santosh (2017) with some updates. Laurentia-Siberia are placed in a similar configuration to that in figure 14b (1.77 Ga). Australia is located off present-day western Laurentia in a position consistent with Columbia/Nuna models. The southern Indian blocks are located near the North China craton and Baltica and Amazonia are positioned off the present-day east coast of Laurentia.

Late Mesoproterozoic-Neoproterozoic Poles

There are only two reliable poles from India during this time interval and they are separated by nearly 300 million years (Table 1). Li et al. (2008) provide a series of paleogeographic reconstructions of Rodinia at 1.1 Ga, 1.05 Ga and 1.0 Ga with India placed adjacent to East Antarctica in a traditional East Gondwana configuration. In the Li et al. (2008) model, India shows a large latitudinal shift from polar latitudes at 1.1 Ga (Fig. 15a) to lower latitudes by 1.0 Ga. The position of India at 1.05 Ga appears to be tied to the poorly-constrained Wajrakur Kimberlite virtual geomagnetic pole (Miller and Hargraves, 1994) and otherwise follows the known rapid movement of Laurentia during the same time interval. In contrast, our mean 1.073 Ga pole places India very close to the equator (Fig. 15a) and the available paleomagnetic poles from 1.1-1.0 Ga (Mahoba dyke, Majhgawan kimberlite and Bhander-Rewa sedimentary rocks) suggest very little latitudinal motion. In addition, the 0.77-0.75 Ga Malani Igneous Complex pole (Meert et al., 2013; Table 1) along with coeval data from Australia (Fig. 15b; Wingate et al., 2000; Li, 2000) suggest that a long-lived East Gondwana configuration is incompatible with paleomagnetic data. We therefore view the Li et al. (2008) reconstructions of India within Rodinia with skepticism.

Conclusions

We have compiled (in a separate manuscript) all of the published paleomagnetic poles from Peninsular India. Only eleven poles were selected for this paper that meet stringent criteria required to test a variety of paleogeographic issues. Based on our current knowledge, Peninsular India represents an amalgam of five or six regions known as the Dharwar, Bastar, Singhbhum, Bundelkhand cratons, Aravalli-Banded Gneiss Complex and Marwar terrane. The Bundelkhand craton, Marwar terrane and Aravali-BGC (North Indian Blocks-NIB) are separated from the other three blocks (South Indian Blocks-SIB) by an ENE-WSW trans-continental belt known as the Central Indian Tectonic Zone (CITZ). The CITZ was affected by several tectonothermal events culminating with a Himalayan-style collision between 1.1 to 0.9 Ga. Paleomagnetic and geochronological data from these regions suggest that the SIB were in contact no later than 1.765 Ga and that Peninsular India was fully assembled between 1.1-0.9 Ga.

A time-series picture of Peninsular India's cratonic nuclei is evaluated at discrete intervals. Although useful, they provide limited constraints on India's location in the Columbia and Rodinia supercontinents. A more robust paleogeographic picture at 1.88 Ga indicates that neither Columbia/Nuna nor India were fully assembled. A second time-slice at 1.45 Ga is compatible with the existence of a large landmass (Columbia) with the Southern Indian Blocks located either near the Congo-Sao Francisco craton margin or in close proximity to Australia and the North China Craton. Given the ambiguities of paleomagnetic data and the lack of a lengthy APWP for Peninsular India, these time slices should be viewed with caution. We note several problems with the position of India between 1.1-1.0 Ga in some existing maps of Rodinia (Li et al., 2008). We further argue that the paradigm of an intact East Gondwana for most of the Proterozoic is problematic (see also Meert, 2003; Meert, 2014). Lastly, we note that India contains a wealth of untapped 'paleogeographic resources' that promise to provide an improved picture of India's place in Precambrian supercontinents in the coming years.

Our paleomagnetic data are compatible with tectonic models that posit a final 1.0-0.9 Ga assembly of Peninsular India (Bhowmik et al., 2019) although an earlier 1.6-1.5 Ga 'close approach' between the SIB/NIB cannot be tested with the extant paleomagnetic data.

Acknowledgements: This research was supported by grants from the USA National Science Foundation to JGM (EAR18-50693, EAR13-47942, EAR09-10888). The conclusions and interpretations offered in this publication are those of the authors and do not reflect the opinions of the funding agency. We thank Elisa Piispa, Lauri Pesonen and an anonymous review for careful and thought-provoking comments on the initial draft.

References Cited

Antonio, P. Y., D'Agrella-Filho, M. S., Trindade, R. I., Nédélec, A., de Oliveira, D. C., da Silva, F. F., Lana, C., 2017. Turmoil before the boring billion: paleomagnetism of the 1880–1860 Ma Uatumã event in the Amazonian craton. Gondwana Research, 49, 106-129.

Athavale, R.N., Radhakrishnamurthy, C., Sahasrabudhe, P.W., 1963. Paleomagnetism of some Indian rocks. Geophysical Journal International, 7, 304-313.

Athavale, R. N., Hansraj, A., Verma, R. K., 1972. Palaeomagnetism and age of Bhander and Rewa sandstones from India. Geophysical Journal International, *28*, 499-509.

Babu, N. R., Venkateshwarlu, M., Shankar, R., Nagaraju, E., & Parashuramulu, V., 2018. New paleomagnetic results on 2367 Ma Dharwar giant dyke swarm, Dharwar craton, southern India: implications for Paleoproterozoic continental reconstruction. Journal of Earth System Science, 127, https://doi.org/10.1007/s12040-017-0910-3.

Balakrishnan, S., Rajamani, V., Hanson, G.N., 1999. U-Pb Ages for Zircon and Titanite from the Ramagiri Area, Southern India: Evidence for Accretionary Origin of the Eastern Dharwar Craton during the Late Archean. Journal of Geology, 107, 69-86.

Bandyopadhyay, B. K., Bhoskar, K. G., Ramachandra, H. M., Roy, A., & Khadse, V. K., 1990. Recent geochronological studies in parts of the Precambrian of central India. Visesa Prakasana-Bharatiya Bhuvaijñanika Sarveksana, 28, 199-210.

Basu A, Bickford M.E., 2015. An alternate perspective on the opening and closing of the Intracratonic Purana Basins in Peninsular India. Journal Geological Society India, 85, 5–25.

Bates, M.P. and Jones, D.L., 1996. A paleomagnetic investigation of the Mashonland dolerites, north-east Zimbabwe, Geophysical Journal International, 126, 513-524.

Belica, M.E., Piispa, E.J., Meert, J.G., Pesonen, L.J., Plado, J., Pandit, M.K., Kamenov, G.D., Celestino, M., 2014. Paleoproterozoic mafic dyke swarms from the Dharwar craton; paleomagnetic poles for India from 2.37-1.88 Ga and rethinking the Columbia supercontinent. Precambrian Research, 244, 100-122.

Bhalla, M. S., Hansraj, A., Prasad Rao, N.T.V., 1980. Paleomagnetic studies of Bangarpet and Sargur dykes of Precambrian age from Karnataka, India. Geoviews, 8, 181-189.

Bhattacharya, H. N., Nelson, D. R., Thern, E. R., Altermann, W., 2015. Petrogenesis and geochronology of the Arkasani Granophyre and felsic Dalma volcanic rocks: implications for the evolution of the Proterozoic North Singhbhum Mobile Belt, east India. Geological Magazine 152, 492-503.

Bhowmik, S.K., 2019. The current status of orogenesis in the Central Indian Tectonic Zone: a view from its southern margin. Geological Journal, 54, 2912-2934.

Bhowmik, S.K., Chattopadhyay, A., Gupta, S., Dasgupta, S., 2012a. Proterozoic tectonics: An Indian perspective the Central Indian Tectonic Zone (CITZ). Proceedings of the Indian National Scientific Academy, 78, 385-391.

Bhowmik, S.K., Wilde, S.A., Bhandari, A., Pal, T., Pant, N.C., 2012b. Growth of the greater Indian landmass and its assembly in Rodinia: geochronological evidence from the Central Indian Tectonic Zone. Gondwana Research, 22, 54-72.

Biggin, A.J., Strik, G.H.M.A., Langereis, C., 2008. Evidence for a very-long-term trend in geomagnetic secular variation. Nature Geosciences, 1, 395-398.

Bispos-Santos, F., D'Agrella-Filho, M.S., Trindade, R.I.F., Elming, S.Å., Janikian, L., Vasconcelos, P.M., Perillo, B..M., Pacca, I.I.G., da Silva, J.A., Barros, M.A.S., 2012. Tectonic implications of the 1419 Ma Nova Guarita mafic intrusives paleomagnetic pole (Amazonian craton) on the longevity of Nuna. Precambrian Research, 196-197.

Bispos-Santos, F., D'Agrella-Filho, M. S., Trindade, R. I.F., Janikian, L., Reis, N. J., 2014. Was there SAMBA in Columbia? Paleomagnetic evidence from 1790 Ma Avanavero mafic sills (northern Amazonian Craton). Precambrian Research, 244, 139-155.

Bogdanova, S.V., Gorbatschev, R., Garetsky, R.G., 2016. EUROPE East European craton. Reference Module on Earth Systems and Environmental Sciences. Elsevier Publications doi.org/10.1016/B978-0-12-409548-9.10020-X.

Bose, M.K., 2008. Petrology and geochemistry of Proterozoic 'Newer Dolerite' and associated ultramafics within Singhbhum granite pluton, eastern India. in: Srivastava, R.K., Shivaji, Ch., and Chalapathi Rao, V. (eds). Indian Dykes: Geochemistry, Geophysics and Geochronology: Narosa, New Delhi, 413-446.

Brown, M. C., Torsvik, T.H., Pesonen, L.J., 2018. Nordic workshop takes on major puzzles of paleomagnetism. Eos, 99, https://doi.org/10.1029/2018EO094671

Buchan, K. L., Mortensen, J. K., Card, K. D., 1993. Northeast-trending Early Proterozoic dykes of southern Superior Province: multiple episodes of emplacement recognized from integrated paleomagnetism and U–Pb geochronology. Canadian Journal of Earth Sciences, 30, 1286-1296.

Buchan, K. L., Mertanen, S., Park, R. G., Pesonen, L. J., Elming, S. Å., Abrahamsen, N., Bylund, G., 2000. Comparing the drift of Laurentia and Baltica in the Proterozoic: the importance of key palaeomagnetic poles. Tectonophysics, 319, 167-198.

Buchan, K. L., LeCheminant, A. N., & van Breemen, O., 2012. Malley diabase dykes of the Slave craton, Canadian Shield: U–Pb age, paleomagnetism, and implications for continental reconstructions in the early Paleoproterozoic. Canadian Journal of Earth Sciences, 49, 435-454.

Buchan, K. L., Mitchell, R. N., Bleeker, W., Hamilton, M. A., & LeCheminant, A.N., 2016. Paleomagnetism of ca. 2.13–2.11 Ga Indin and ca. 1.885 Ga Ghost dyke swarms of the Slave craton: Implications for the Slave craton APW path and relative drift of Slave, Superior and Siberian cratons in the Paleoproterozoic. Precambrian Research, 275, 151-175.

Cawood, P.A., Korsch, R.J., 2008. Assembling Australia: Proterozoic building of a continent. Precambrian Research 166, 1–38

Chakraborty, P.P., Saha S., Das, P., 2015. Geology of the Mesoproterozoic Chhattisgarh Basin, central India: current status and future goals, Geological Society of London Memoir, 43, 185-205.

Clark, D.A., 1982. Preliminary paleomagnetic results from the Cuddapah traps of Andrha Pradesh. Monograph-2, On Evolution of the intracratonic Cuddapah Basin. HPG,Hyderabad, India, 47–51.

Collins, A.S., Clark, C., Plavsa, D., 2014. Peninsular India in Gondwana: The tectonothermal evolution of the Southern Granulite Terrane and its Gondwana counterparts, Gondwana Research, 14, 190-203.

Cox, A., 1969. Confidence limits for the precision parameter κ. Geophysical Journal of the Royal Astronomical Society, 18, 545-549.

Dasgupta, S., Bose, S., Bhowmik, S.K., Sengupta, P., 2017. The Eastern Ghats Belt India, in the context of supercontinent assembly. Geological Society of London Special Publication 457, 87-104.

Dash, J. K., Pradhan, S. K., Bhutani, R., Balakrishnan, S., Chandrasekaran, G., Basavaiah, N., 2013. Paleomagnetism of ca. 2.3 Ga mafic dyke swarms in the northeastern Southern Granulite Terrane, India: Constraints on the position and extent of Dharwar craton in the Paleoproterozoic. Precambrian Research, 228, 164-176.

Davis, J.K., Meert, J.G., Pandit, M.K., 2014. Paleomagnetic analysis of the Marwar Supergroup, Rajasthan, India and proposed intrabasinal correlation. Journal of Asian Earth Sciences, 91, 339-351.

Dawson, E.M., Hargraves, R.B., 1994, Paleomagnetism of Precambrian swarms in the Harohalli area, south of Bangalore, India. Precambrian Research, 69, 157–167.

Deb, M., 1999. Metallic mineral deposits of Rajasthan in P. Kataria (Ed.), Proceedings Seminar on Geology of Rajasthan– Status and Perspective, M.L. Sukhadia University, Udaipur, India, 213-237.

Deb, M., Thorpe, R.I., 2004. Geochronological constraints in the Precambrian geology of Rajasthan and their metallogenic implications. in: M. Deb, W.D. Goodfellow (eds.), Sediment-hosted Lead–zinc Sulphide Deposits. Narosa Publishing House, New Delhi, pp. 246-263

Deb, M., Thorpe, R.I., Krstic, D., Corfu, F. and Davis, D.W., 2001. Zircon U-Pb and galena Pb isotopic evidence for an approximate 1.0 Ga terrane constituting the western margin of the Aravalli-Delhi orogenic belt, northwestern India. Precambrian Research, 108, 195-213.

De Kock, M.O., Evans, D.A.D., Dorland, H.C., Beukes, N.J., Gutzmer, J., 2006. Paleomagnetism of the lower two unconformity-bounded sequences of the Waterberg Group, South Africa: Towards a better-defined apparent polar wander path for the Paleoproterozoic Kaapvaal craton. South African Journal of Geology, 109, 157-182.

De Kock, M.O., Beukes, N.J., Mukhopadhyay, J., 2015. Paleomagnetism of Mesoproterozoic limestone and shale successions of some Purana basins in southern India. Geological Magazine, 152, 728-750.

Deenen, M.H.L., Langereis, C., van Hinsbergen, D.J.J., Biggin, A.J., 2011. Geomagnetic secular variation and the statistics of paleomagnetic directions. Geophysical Journal International, 186, 509-520.

Deenen, M.H.L., Langereis, C., van Hinsbergen, D.J.J., Biggin, A.J., 2014. Erratum:Geomagnetic secular variation and the statistics of paleomagnetic directions. Geophysical Journal International, 197, 643.

Demirer, K., 2012. U-Pb baddeleyite ages from the mafic dyke swarms in Dharwar craton, India: links to ancient supercontinent, M.Sc. Thesis Lund University, Lund, Sweden, 308 pp.

Didenko, A.N., Vodovov, V.Y., Pisarevsky, S.A., Gladkochub, D.P., Donskaya, T.V., Mazukabzov, A.M., Stanovich, A.M., Bibikova, E.V., Kirnozova, T.I., 2009. Paleomagnetism and U-Pb dates of the Paleoproterozoic Atikan Group (South Siberia) and implications for pre-Neoproterozoic tectonics, Geological Society of London Special Publication, 323, 145-163.

Didenko, A.N., Vodovozov, V.Yu., Peskov, A.Yu., Guryanov, V.A., Kosynkin, A.V., 2015. Paleomagnetism of the Ulkan massif (SE Siberian platform) and theapparent polar wander path for Siberia in late Paleoproterozoic–early Mesoproterozoic times. Precambrian Research, 259, 58-77.

Elming, S.Å., 1994. Paleomagnetism of Precambrian rocks in northern Sweden and its correlation to radiometric data, Precambrian Research, 69, 61-79.

Elming, S.Å., Moakhar, M.O., Layer, P., Donadini, F., 2009. Uplift deduced from remanent magnetization of a Proterozoic basic dyke and the baked country rock in the Hotting area, Central Sweden: a paleomagnetic and $^{40}Ar/^{39}Ar$ study. Geophysical Journal International, 179, 59-78.

Elming, S.Å., Shumlyansky, L., Kravchenko, S., Layer, P., Söderlund, U., 2010. Proterozoic basic dykes in the Ukrainian Shield: A paleomagnetic, geochronologic and geochemical study—the accretion of the Ukrainian Shield to Fennoscandia. Precambrian Research, 178, 119-135.

Elston, D.P., Enkin R.J., Baker, J., Kisilevsky, D.K., 2002. Tightening the Belt: Paleomagnetic-stratigraphic constraints on deposition, correlation, and deformation of the Middle Proterozoic (ca. 1.4 Ga) Belt-Purcell Supergroup, United States and Canada. Geological Society of America Bulletin, 114, 619-638.

Emslie, R.F., Irving, E., Park, J.K., 1976. Further paleomagnetic results from the Michikamau intrusion, Labrador. Canadian Journal of Earth Sciences, 13 1052-1057.

Evans, M.E., 1968. Magnetization of dikes: a study of the paleomagnetism of the Widgiemooltha dile suite, western Australia, Journal of Geophysical Research, 73, 33361-33270.

Evans, D. A. D., & Halls, H. C., 2010. Restoring Proterozoic deformation within the Superior craton. Precambrian Research, 183, 474-489.

Evans, D.A.D., Veselovsky, R.V., Petrov, P.Yu., Shatsillo, A.V., Pavlov, V.E., 2016. Paleomagnetism of Mesoproterozoic margins of the Anabar Shield: a hypothesized billion-year partnership of Siberia and northern Laurentia, Precambrian Research, 281, 639-655.

Fahrig, W.F., Bridgwater, D., 1976. Late Archean-Early Proterozoic paleomagnetic pole positions from West Greenland. in The Early History of the Earth, (ed) Windley, B.F., John Wiley & Sons, London, 427-439.

Fisher, R. A., 1953. Dispersion on a sphere. Proceedings of the Royal Society of London. Series A. Mathematical and Physical Sciences, 217, 295-305.

French, J.E., Heaman, L.M., Chacko, T., Srivastava, R.K., 2008. 1891-1883 Ma southern Bastar craton-Cuddapah mafic igneous events, India: a newly recognized large igneous province. Precambrian Research, 160, 308–322.

French, J.E., Heaman, L.M., 2010. Precise U-Pb dating of Paleoprotoerozoic mafic dyke swarms of the Dharwar craton, India: Implications for the existence of the Neoarchean supercraton Sclavia. Precambrian Research, 183, 416–441.

Ghosh, J. G., 2004. 3.56 Ga tonalite in the central part of the Bastar craton, India: oldest Indian date. Journal of Asian Earth Sciences, 23, 359-364.

Gladkochub, D., Pisarevsky, S., Donskaya, T., Natapov, L., Mazukabov, A., Stanevich, A.,Sklyarov, E., 2006. The Siberian craton and its evolution in terms of the Rodinia hypothesis. Episodes 29, 169–174.

Gregory, L.C., Meert, J.G., Bingen, B.H. Pandit, M.K. and Torsvik, T.H., 2008. Paleomagnetic and geochronologic study of Malani Igneous suite, NW India: implications for the configuration of Rodinia and the assembly of Gondwana. Precambrian Research, 170, 13-26.

Gregory, L.C., Meert, J.G., Pandit, M.K., Pradhan, V.R., Endale, T., Malone, S.J., 2006. A paleomagnetic and geochronologic study of the Majhgawan kimberlite, India: Implications for the age of the Upper Vindhyan Supergroup. Precambrian Research, 149, 65-75.

Gopalan, K., & Kumar, A., 2008. Phlogopite K–Ca dating of Narayanpet kimberlites, south India: implications to the discordance between their Rb–Sr and Ar/Ar ages. Precambrian Research, 167, 377-382.

Gopalan, K., Kumar, A., Kumar, S., Vijayagopal, B., 2013. Depositional history of the Upper Vindhyan succession, central India: time constraints from Pb–Pb isochron ages of its carbonate components. Precambrian Research, 233, 108-117.

Gumsley, A.P., Chamberlain, K.R., Bleeker, W., Söderlund, U., de Kock, M.O., Larsson, E.R., Bekker, A., 2017. Timing and tempo of the Great Oxidation Event, Proceedings of the National Academy of Sciences, 114, 1811-1816.

Gupta, S.N., Arora, Y.K., Mathur, R.K., Iqbaluddin, Prasad, B., Sahai, T.N., Sharma, S.B., 1997. The Precambrian geology of the Aravalli region, Southern Rajasthan and north-eastern Gujarat, India (with geological map, Scale 1:250 000), Memoirs of the Geological Survey of India, 123, 262 pp.

Halls, H.C., Li, J., Davis, D., Hou, G., Zhang, B., Qian X., 2000. A precisely dated Proterozoic paleomagnetic pole from the North China Craton and its relevance to paleocontinental reconstructions. Geophysical Journal International, 143, 185-203.

Halls, H.C., Kumar, A., Srinivasan, R., Hamilton, M.A., 2007. Paleomagnetism and U-Pb geochronology of easterly trending dykes in the Dharwar craton, India: feldspar clouding, radiating dyke swarms and the position of India at 2.37 Ga, Precambrian Research, 155, 47-68.

Harlan S.S., Geissman, J.W., Snee, L.W., 2008. Paleomagnetism of Proterozoic mafic dykes from the Tobacco Root mountains, southwest Montana, Precambrian Research, 163, 239-264.

Hasnain, I., Qureshy, M. N., 1971. Paleomagnetism and geochemistry of some dikes in Mysore State, India. Journal of Geophysical Research, 76, 4786-4795.

Heslop, D., Roberts, A.P., 2018. Revisiting the paleomagnetic reversal test: A Bayesian hypothesis testing framework for a common mean direction, Journal of Geophysical Research Solid Earth, 123, 7225-7236.

Hoffman, P.F., 1997. Tectonic genealogy of North America. in: van der Pluijm, B.A., Marshak, S. (eds.), Earth Structure: An Introduction to Structural Geology and Tectonics. McGraw-Hill, New York, 459–464.

Hoffman, P.F., Schrag, D.P., 2002. The Snowball Earth Hypothesis: testing the limits of global change. Terra Nova, 14, 129-155.

Hoffman, P.F., Abbot, D.S., Ashkenazy, Y., Benn, D.I., Brocks, J.J., Cohen, P.A., Cox, G.M., Creveling, J.R., Donnadieu, Y., Erwin, D.H., Fairchild, I.J., Ferreira, D., Goodman, J.C., Halverson, G.P., Jansen, M.F., Le Hir, G., Love, G.D., Macdonald, F.A., Maloof, A.C., Partin, C.A., Ramstein, G., Rose, B.E.J., Rose, C.V., Sadler, P.M., Tziperman, E., Voigt, A. and Warren, S.G., 2017. Snowball Earth climate dynamics and Cryogenian geology-geobiology. Science Advances, 3, p.e1600983.

Humbert, F., Sonnette, L., De Kock, M. O., Robion, P., Horng, C. S., Cousture, A., Wabo, H., 2017. Palaeomagnetism of the early Palaeoproterozoic, volcanic Hekpoort Formation (Transvaal Supergroup) of the Kaapvaal craton, South Africa. Geophysical Journal International, 209, 842-865.

Irving,E., McGlynn,J.C., 1979. Palaeomagnetism in the Coronation Geosyncline and arrangements of continents in the middle Proterozoic. Geophysical Journal of the Royal Astronomical Society, 58, 309-336.

Irving, E., Baker, J., Hamilton, M., Wynne, P. J., 2004. Early Proterozoic geomagnetic field in western Laurentia: implications for paleolatitudes, local rotations and stratigraphy. Precambrian Research 129, 251-270.

Killian, T.M., Chamberlain, K.R., Evans, D.A.D., Bleeker, W., Cousens, B.L., 2016. Wyoming on the run—toward a final Paleoproterozoic assembly of Laurentia. Geology, 44, 863-866.

Klein, R., Pesonen, L. J., Mänttäri, I., Heinonen, J. S., 2016. A late Paleoproterozoic key pole for the Fennoscandian Shield: A paleomagnetic study of the Keuruu diabase dykes, Central Finland. Precambrian Research, 286, 379-397.

Klootwijk, C. T., 1973. Palaeomagnetism of upper Bhander sandstones from central India and implications for a tentative Cambrian Gondwanaland reconstruction. Tectonophysics, 18, 123-145.

Klootwijk, C. T., 1975. A note on the palaeomagnetism of the late Precambrian Malani Rhyolites near Jodhpur-India. Journal of Geophysics, 41, 189-200.

Kumar, A., Bhalla, M.S., 1983, Paleomagnetics and igneous activity of the area adjoining the southwestern margin of the Cuddapah basin, India, Geophysical Journal of the Royal Astronomical Society, 73, 27–37.

Kumar, A. (2001). Rb-Sr ages of kimberlites and lamproites from Eastern Dharwar craton, South India. Journal of the Geological Society of India, 58, 135-142.

Kumar, A., Heaman, L. M., Manikyamba, C., 2007. Mesoproterozoic kimberlites in south India: A possible link to~ 1.1 Ga global magmatism. Precambrian Research, 154, 192-204.

Kumar, A., Nagaraju, E., Besse, Jean, Rao, Y.J. Bhaskar, 2012a. New age, geochemical and paleomagnetic data on a 2.21 Ga dyke swarm from south India: Constraints on Paleoproterozoic reconstruction, *Precambrian Research*, 220–221, 123–138.

Kumar, A., Hamilton, M.A., Halls, H.C., 2012b. A Paleoproterozoic giant radiating dyke swarm in the Dharwar craton, southern India, Geochemistry Geophysics Geosystems, 13, http://dx.doi.org/10.1029/2011GC003926.

Kumar, A., Nagaraju, E., Srinivasa Sarma, D., Davis, D.W., 2014. Precise Pb baddeleyite geochronology by the thermal extraction-thermal ionization mass spectrometry method. Chemical Geology, 372, 72–79.

Kumar, A., Parashuramulu, V., Nagarju, E., 2015. A 2082 Ma radiating dyke swarm in the Eastern Dharwar craton, southern India and its implications to Cuddapah basin formation. Precambrian Research, 266, 490-505.

Kumar, A., Parashuramulu, V., Shankar, R., Besse, J., 2017. Evidence for a Neoarchean LIP in the Singhbhum craton, eastern India: Implications to Vaalbara supercontinent. Precambrian Research, 292, 163-174.

Leelanandam, C., Burke, K., Ashwal, L.D., Webb, S., 2006. Proterozoic mountain building in Peninsular India: An analysis based primarily on alkaline igneous rock distribution. Geological Magazine, 143, 1-18.

Letts,S., Torsvik, T.H., Webb, S.J., Ashwal, .D., 2009. Palaeomagnetism of the 2054 Ma Bushveld Complex (South Africa): implications for emplacement and cooling. Geophysical Journal International, 179, 850-872.

Li, Z.X. (2000) Paleomagnetic evidence for unification of the North and West Australian cratons by 1.7 Ga: new results from the Kimberley Basin of northwestern Australia. Geophysical Journal International, 142, 173-180.

Li, Z.X., Bogdanova, S.V., Davidson, A., Collins, A.S., De Waele, B., Ernst, R.E., Fitzsimons, I.C.W., Fuck, R.A., Gladkochub, D.P., Jacobs, J., Karlstrom, K.E., Lu, S., Natapov, L.M., Pease, V., Pisarevsky, S.A., Thrane, K., Vernikovsky, V., 2008. Assembly, configuration, and break-up history of Rodinia: A synthesis. Precambrian Research, 160, 179-210.

Liao, A.C-Y., Shellnutt, J.G., Hari, K.R., Denyszyn, S.W., Vishwakarma, N., Verma, C.B., 2019. A petrogenetic relationship between bonititic dyke swarms of the Indian shield: Evidence from the central Bastar Craton and the NE Dharwar craton, Gondwana Research, 69, 193-211.

Lubnina, N., Ernst, R., Klausen, M., & Söderlund, U., 2010a. Paleomagnetic study of NeoArchean–Paleoproterozoic dykes in the Kaapvaal Craton. Precambrian Research, 183, 523-552.

Lubnina, N.V., Mertanen, S., Söderlund, U., Bogdanova, S., Vasilieva, T.I., Frank-Kamenetsky, D., 2010b. The East European Craton in the Mesoproterozoic: New Key Paleomagnetic Poles. Precambrian Research, 183, 442-462.

Mahadevan, T.M., 2002. Geology of Bihar and Jharkhand. Geological Society of India, Bangalore. 563 pp.

Malone, S.J., Meert, J.G., Banerjee, D.M., Pandit, M.K., Tamrat, E., Kamenov, G.D., Pradhan, V.R., Sohl, L.E., 2008. Paleomagnetism and detrital zircon geochronology of the Upper Vindhyan sequence, Son Valley and Rajasthan, India: A ca. 1000 Ma closure age for the Purana basins? Precambrian Research, 164, 137159.

McElhinny, M.W., Cowley, J., Edwards, D.J., 1978. Paleomagnetism of some rocks from Peninsular India and Kashmir. Tectonophysics, 50, 41-54.

McElhinny, M.W., McFadden, P.L., 1997. Paleosecular variation over the past 5 million Myr. based on a new generalized database. Geophysical Journal International, 131, 240-252.

McFadden, P.L., McElhinny, M.W., 1990. Classification of the reversal test in paleomagnetism. Geophysical Journal International, 103, 725-729.

McFadden, P., Merrill, R., McElhinny, M., Lee, S., 1991. Reversals of the Earth's magnetic field and temporal variations of the dynamo families. *Journal of Geophysical Research Solid Earth*, 96, 3923–3933.

McKenzie, N. R., Hughes, N. C., Myrow, P. M., Xiao, S., and Sharma, M., 2011. Correlation of Precambrian-Cambrian sedimentary successions across northern India and the utility of isotopic signatures of Himalayan lithotectonic zones. Earth and Planetary Science Letters, 312, 471-483.

McKenzie, N.R., Hughes, N.C., Myrow, P.M., Banerjee, D.M., Deb, M., Planavsky, N.J., 2013. New age constraints for the Proterozoic Aravalli–Delhi successions of India and their implications. Precambrian Research, 238, 120 – 128.

McMenamin, M.A.S., McMenamin, D.L.S., 1990. The Emergence of Animals: The Cambrian Breakthrough. Columbia University Press, New York, 217 pp.

Mitchell,R.N., Hoffman,P.F., Evans,D.A.D, 2010. Coronation loop resurrected: Oscillatory apparent polar wander of Orosirian (2.05–1.8 Ga) paleomagnetic poles from Slave craton., Precambrian Research, 179, 121-134.

Mitchell, R.N., Bleeker, W., Van Breemen, O., LeCheminant, A.N., Peng, P., Nilsson, M.K.M., Evans, D.A.D., 2014. Plate tectonics before 2.0 Ga: Evidence from paleomagnetism of cratons within supercontinent Nuna. American Journal of Science, 314, 878-894.

Meert, J.G. 2002. Paleomagnetic evidence for a Paleo-Mesoproterozoic supercontinent Columbia, Gondwana Research, 5, 207-215.

Meert, J.G., 2003. A synopsis of events related to the assembly of eastern Gondwana, Tectonophysics, 362, 1-40.

Meert, J.G., 2012. What's in a name? The Columbia (Palaeopangea/Nuna) Supercontinent. Gondwana Research, 21, 987-993.

Meert, J.G., 2014. Strange Attractors, Spiritual Interlopers and Lonely Wanderers: The Search for Pre-Pangæan Supercontinents. Geoscience Frontiers, 5, 155-166.

Meert, J.G. and Stuckey, W., 2002. Paleomagnetism of the St. Francois Mountains, Missouri revisited, Tectonics, 21, doi:10.1029/2000TC001265.

Meert, J.G., Torsvik, T.H., 2003. The making and unmaking of a supercontinent: Rodinia revisited. Tectonophysics, 375, 261-288.

Meert, J.G., Pandit, M.K., 2015. Precambrian Evolution of Peninsular India and its Link to Basin evolution, in: Eriksson et al. (eds) *Geological Society of London, Special Publication #43*, Precambrian Basins of India: Stratigraphic and Tectonic Criteria, pp. 29-54.

Meert, J.G., Santosh, M., 2017. The Columbia supercontinent revisited. Gondwana Research, 50, 67-83.

Meert, J.G., Pandit, M.K., Pradhan, V.R., Banks, J.C., Sirianni, R., Stroud, M., Newstead, B., Gifford, J., 2010. The Precambrian tectonic evolution of India: A 3.0 billion year odyssey. Journal of Asian Earth Sciences, 39, 483-515.

Meert, J.G., Pandit, M.K., Pradhan, V.R., Kamenov, G.D., 2010. Preliminary report on the paleomagnetism of 1.88 Ga dykes from the Bastar and Dharwar cratons. Gondwana Research, 20, 335-343.

Meert, J.G., Pandit, M.K., Kamenov, G.D., 2013. Further geochronological and paleomagnetic constraints on Malani (and pre-Malani) magmatism in NW India. Tectonophysics, 608, 1254-1267.

Meert, J.G., Pandit, M.K., Pivarunas, A., Katusin, K., Sinha, A.K., 2017. India and Antarctica in the Precambrian: A brief analysis, Geological Society of London Special Publication 457, 339-352.

Mertanen, S., Hölttä, P., Pesonen, L.J., Paavola, J., 2006. Paleomagnetism of Paleoproterozoic dykes in central Finland. In: Hansli et al. (eds) Dyke Swarms-Time Markers of crustal evolution, Taylor and Francis, London. Pp 243-256.

Miller, K.C., Hargraves, R.B., 1994. Paleomagnetism of some Indian kimberlites and lamproites. Precambrian Research, 69, 259-267.

Miller, S.R., Mueller, P.A., Meert, J.G., Kamenov, G.D., Pivarunas, A.F., Sinha, A.K., Pandit, M.K., 2018. Detrital Zircons Reveal Evidence of Hadean Crust in the Singhbhum Craton, India. Journal of Geology, 126, 541-552.

Misra, S., Johnson, P. T., 2005. Geochronological constraints on evolution of Singhbhum mobile belt and associated basic volcanics of eastern Indian shield. Gondwana Research, 8, 129-142.

Mitchell,R.N., Hoffman,P.F., Evans,D.A.D., 2010. Coronation loop resurrected: Oscillatory apparent polar wander of Orosirian (2.05–1.8 Ga) paleomagnetic poles from Slave craton., Precambrian Research, 179, 121-134.

Mohanty, S., 2015. Paleoproterozoic supracrustals of the Bastar craton: Dongargarh Supergroup and Sausar Group, Geological Society Memoirs, 43, 151-164.

Morgan, G.E., 1985. The paleomagnetism and cooling history of metamorphic and igneous rocks from the Limpopo Belt, southern Africa. Bulletin of the Geological Society of America, 96, 663-675.

Mukhopadhyay, D., 2001. The Archaean Nucleus of Singhbhum: The Present State of Knowledge. Gondwana Research, 4, 307-318.

Naganjaneyulu, K., Santosh, M., 2010. The Central Indian Tectonic Zone: a geophysical perspective on continental amalgamation along a Mesoproterozoic suture. Gondwana Research, 18, 547-564.

Nagaraju, E., Parashuramulu, V., Babu, N.R., Narayana, A.C., 2018a. A 2207 Ma radiating mafic dyke swarm from eastern Dharwar craton, Southern India: Drift history through Paleoproterozoic. Precambrian Research, 317, 89-100.

Nagaraju, E., Parashuramulu, V., Kumar, A., Sarma, D.S., 2018b. Paleomagnetism and geochronological studies on a 450 km long 2216 Ma dyke from the Dharwar craton, South India. Physics of the Earth and Planetary Interiors, 274, 222-231.

Naqvi, S.M., Rogers, J.J.W., 1987. Precambrian Geology of India. Oxford University Press, Oxford, pp. 223.

Neuvonen, K.J., Korsman, K., Kouvo, O., Paavola, J., 1981. Paleomagnetism and age relations of the rocks in the Main Sulphide Ore Belt in central Finland. Bulletin of the Geological Society of Finland, 53, 109-133.

Patranabis-Deb, S.; Bickford, M. E.; Hill, B.; Chaudhuri, A. K.; and Basu, A. 2007. SHRIMP ages of zircon in the uppermost tuff in Chattisgarh Basin in central India require ~500-Ma adjustment in Indian Proterozoic stratigraphy. Journal of Geology, 115, 407–415.

Pehrsson, S.J., Eglington, B.M., Evans, D.A.D., Huston, D. & Reddy, S.M., 2015. Metallogeny and its link to orogenic style during the Nuna supercontinental cycle. Geological Society Special Publication, 424, 83-94.

Pesonen, L. J., Romu, I., Piispa, E., Dongre, A. N., Klein, R., 2012. Paleomagnetic results of Wajrakur kimberlites and other mafic dykes, Dharwar craton, India. Abstract Volume Supercontinent Symposium, Helsinki, Finland Abstracts, 108-110.

Piispa, E.J., Smirnov, A.V., Pesonen, L.J., Lindgadevaru, M., Anantha-Murthy, K.S., Devaraju, T.C., 2011. An integrated study of Proterozoic dykes, Dharwar craton, southern India, in Srivastava, R.J. (ed) *Dyke Swarms: Keys for Geodynamic Interpretation*, Springer Publishing, New York, pp. 73-93.

Pisarevsky, S.A., Sokolov, S.J., 2001. The magnetostratigraphy and a 1780 Ma paleomagnetic pole from the red sandstones of the Vazhinka River section, Karelia, Russia. Geophysical Journal International, 146, 531-538.

Pisarevsky, S.A., Bylund, G., 2010. Paleomagnetism of the 1780–1770 mafic and composite intrusions of the Smaland (Sweden): implications for the Mesoproterozoic supercontinent. American Journal of Science 310, 1168–1186.

Pisarevsky, S.A., Biswal, T.K., Wang, X-C., de Waele, B., Ernst, R., Söderlund, U., Tait, J.A., Ratre, K., Singh, Y.K., Cleve, M., 2013. Paleomagnetic, geochronological and geochemical study of Mesoproterozoic Lakhna dykes in the Bastar craton, India: Implications for the Mesoproterozoic supercontinent. Lithos, 174, 125-143.

Pisarevsky, S.A., de Waele, B., Jones, S., Söderlund, U., Ernst, R.A., 2014. Paleomagnetism and U-Pb age of the 2.4 Eraynia mafic dykes in the Southwestern Yilgarn, Western Australia: paleogeographic and geodynamic implications. Precambrian Research, 259, 222-231.

Pivarunas, A.F., Katusin, K.D., Meert, J.G., Craver, A., Miller, S.R., Roderus, K., Sinha, A.K., Pandit, M.K., 2018. Magnetization, remagnetization and complication in the Singhbhum craton, India. GSA Abstracts with Programs, 50, doi:10.1130/abs/2018AM-320940.

Pivarunas, A.F., Meert, J.G., Miller, S.R., 2018. Assessing the intersection/remagnetization puzzle with synthetic apparent polar wander paths. Geophysical Journal International, 214, 1164-1172.

Pivarunas, A.F., Meert, J.G., Pandit, M.K., Sinha, A., 2019. Paleomagnetism and geochronology of mafic dykes from the southern granulite terrane, India: Expanding the Dharwar craton southward. Tectonophysics, 760, 4-22.

Pradhan, V.R., Pandit, M.K., Meert, J.G. 2008. A cautionary note on the age of the paleomagnetic pole obtained from the Harohalli dyke swarms, Dharwar craton, southern India. in: Srivastava et al. (eds) *Indian Dykes*, Narosa Publishing House, New Delhi, India, pp. 339-352.

Pradhan, V.R., Meert, J.G., Pandit, M.K., Kamenov, G., Gregory, L.C., Malone, S.J., 2010. India's changing place in global Proterozoic reconstructions: New geochronologic constraints on key paleomagnetic poles from the Dharwar and Aravalli/Bundelkhand cratons. Journal of Geodynamics, 50, 224-242.

Pradhan, V.R., Meert, J.G., Pandit, M.K., Kamenov, G.D., Mondal, M. E.A., 2012. Tectonic evolution of the Precambrian Bundelkhand craton, central India: Insights from paleomagnetic and geochronological studies on the mafic dyke swarms. Precambrian Research, 198-199, 51-76.

Prasad, C.V.R.K., Pulla Reddy, V., Subba Rao, K.V., Radhakrishna Murthy, C., 1987. Palaeomagnetism and the crescent shape of the Cuddapah basin. Geological Society of India Memoirs, 6, 331–347.

Radhakrishna, T., Joseph, M., 1996. Proterozoic palaeomagnetism of the mafic dyke swarms in the high-grade region of southern India. Precambrian Research, 76, 31-46.

Radhakrishna, T., Chandra, R., Srivastava, A.K., Balasubramonian, G., 2013a. Central/Eastern Indian Bundelkhand and Bastar cratons in the Palaeoproterozoic supercontinental reconstructions: a palaeomagnetic perspective, Precambrian Research, 226, 91–104.

Radhakrishna, T., Krishnendu, N., Balasubramonian, G., 2013b. Palaeoproterozoic Indian shield in the global continental assembly: evidence from the palaeomagnetism of mafic dyke swarms. Earth Science Reviews, 126, 370–389.

Rajesh, H. M., Mukhopadhyay, J., Beukes, N. J., Gutzmer, J., Belyanin, G. A., & Armstrong, R. A., 2009. Evidence for an early Archaean granite from Bastar craton, India. Journal of the Geological Society, 166, 193-196.

Ramakrishnan, M., and Vaidyanadhan, R. 2008. Geology of India. Bangalore, Geological Society of India, v1, 552 p.

Rao, V.V., Krishna, V.G., 2013. Evidence for the Neoproterozoic Phulad suture zone and genesis of Malani magmatism in NW India from deep seismic images: Implications for the assembly and breakup of the Rodinia. Tectonophysics, 589, 172-185.

Ratre, K., De Waele, B., Biswal, T. K., Sinha, S., 2010. SHRIMP geochronology for the 1450 Ma Lakhna dyke swarm: Its implication for the presence of Eoarchaean crust in the Bastar Craton and 1450–517 Ma depositional age for Purana basin (Khariar), Eastern Indian Peninsula. Journal of Asian Earth Sciences, 39, 565-577.

Rogers, J.J.W., Santosh, M., 2002. Configuration of Columbia, a Mesoproterozoic supercontinent. Gondwana Research 5, 5–22.

Roy A.B., Jakhar S. R. 2002 Geology of Rajasthan (North-west India) Precambrian to recent. Scientific Publishers (India), Jodhpur 421

Roy, A.B., Purohit, R., 2015. Lithostratigraphic, geochronological ad depositional framework of the Precambrian basins of the Aravalli mountains and adjoining areas, Rajasthan, India. Geological Society of London Special Publication, 43, 55-65.

Sahu, N., Gupta, T., Patel, S. C., Khuntia, D. B. K., Behera, D., Pande, K., & Das, S. K., 2013. Petrology of lamproites from the Nuapada lamproite field, Bastar craton, India. In: *Proceedings of 10th International Kimberlite Conference*, Springer, New Delhi, 137-165.

Sahasrabudhe, P.W., Mishra, D.C., 1966. Paleomagnetism of Vindhyan rocks of India. Bulletin of the National Geophysical Research Institute of India, 4, 49-55.

Salminen, J.M., Evans, D.A.D., Trinade, R.I.F., Oliveira, E.P., Piispa, E.J., Smirnov, A.V., 2016. Paleogeography of the Congo-Sao Francisco craton at 1.5 Ga: expanding the core of the Nuna supercontinent. Precambrian Research, 286, 195-212.

Samal, A.K., Srivastava, R., Sinha, L.K., 2015. ArcGIS studies and field relationships of Paleoproterozoic mafic dyke swarms from the south of Devarakonda area, eastern Dharwar craton, southern India: implications for their relative ages. Journal of Earth Systems Science, 124, 1075-1084.

Santosh, M., Tsunogae, T., Koshimoto, S., 2004. First report of sapphirine-bearing rocks from the Palghat-Cauvery shear zone system, southern India. Gondwana Research, 7, 620-626.

Sarangi, S., Mohanty, S.P., Barik, A., 2017. Rare earth element characteristics of Paleoproterozoic cap carbonates pertaining to the Sausar Group, Central India: Implications for ocean paleoredux conditions. Journal of Asian Earth Sciences, 148, 31-50

Sarkar, S. N., Gopalan, K., Trivedi, J. R., 1981. New data on the geochronology of the Precambrians of Bhandara-Drug, central India. Indian Journal of Earth Sciences, 8, 131-151.

Sarkar, G., Paul, D. K., Misra, V. P., De Laeter, J. R., McNaughton, N. J., 1990). A geochemical and Pb, Sr isotopic study of the evolution of granite-gneisses from the Bastar craton, central India. Journal of the Geological Society of India, 35, 480-496.

Sarkar, G., Corfu, F., Paul, D. K., McNaughton, N.J., Gupta, S. N., & Bishui, P.K., 1993. Early Archean crust in Bastar Craton, Central India—a geochemical and isotopic study. Precambrian Research, 62, 127-137.

Scotese, R.C. and Barrett, S.F., 1990. Gondwana's movement over the South Pole during the Palaeozoic: evidence from lithological indicators of climate. Geological Society, London, Memoirs 12, 75–85.

Schmidt, P.W., Williams, G.E., 2011. Paleomagnetism of the Pandurra Formation and Blue Range beds, Gawler craton, south Australia and the Australian Mesoproterozoic apparent polar wander path. Australian Journal of Earth Sciences, 58, 347-360.

Shankar, R., Sarma, D.S., Babu, N.R., Parashuramulu, V., 2017. Paleomagnetic study of 1765 Ma dyke swarm from the Singhbhum craton: Implications to the paleogeography of India. Journal of Asian Earth Sciences, 157, 235-244.

Shankar, R., Vijayagopal, B., Kumar, A., 2014. Precise Pb-Pb baddeleyite ages of 1765 Ma for Singhbhum 'newer dolerite' dyke swarm. Current Science, 106, 1306-1310.

Sinha Roy, S., Malhotra, G., Mohanty, M., 1998. Geology of Rajasthan. Geological Society of India, Bangalore, 278 pp.

Smirnov, A.V., Evans, D.A., Söderlund, U., Li, Z.X., 2013. Trading partners: Tectonic ancestry of southern Africa and western Australia in Archean supercratons Vaalbara and Zimgarn. Precambrian Research, 224, 11-122.

Söderlund, U., Bleeker, W., Demirer, K., Srivastava, R. K., Hamilton, M., Nilsson, M., Srinivas, M., 2019. Emplacement ages of Paleoproterozoic mafic dyke swarms in eastern Dharwar craton, India: Implications for paleoreconstructions and support for a∼ 30° change in dyke trends from south to north. Precambrian Research, *329*, 26-43.

Srivastava, R.K., Singh, R.K., Verma, R., 2000. Juxtaposition of India and Antarctica During the Precambrian: Inferences from Geochemistry of Mafic Dykes. Gondwana Research, 3, 227-234.

Srivastava, R. K., Hamilton, M. A., & Jayananda, M., 2011. 2.21 Ga large igneous province in the Dharwar Craton, India. In: *International Symposium on Large Igneous Provinces of Asia, Mantle Plumes and Metallogeny, Irkutsk, Russia, Extended Abstract,* 263-266.

Srivastava, R.K., Söderlund, U., Ernst, R.E., Mondal, S.K., Samal, A.K., 2019. Precambrian mafic dyke swarms in the Singhbhum craton (eastern India) and their links with dyke swarms of the eastern Dharwar craton (southern India). Precambrian Research, 329, 23-35.

Stein, H., Hannah, J., Zimmerman, A. & Markey, R., 2006. Mineralization and deformation of the Malanjkhand terrane (2,490–2,440 Ma) along the southern margin of the Central Indian Tectonic Zone. Mineralium Deposita, 40, 755–765.

Stein, H.J., Hannah, J.L., Pandit, M.K., Mohanty, S., Corfu, F., Zimmerman, A., 2014. Molybdenite tricks with titanite give history of the Central Indian Tectonic Zone, *Abstracts EUG General Assembly*, 13209.

Théveniaut, H., Delor, C., Lafon, J.M., Monié, P., Rossi, P., LaLondére, D., 2006. Paleoproterozoic (2155-1970 Ma) evolution of the Guaina Shield (Transamazonina event) in light of new paleomagnetic data from French Guiana. Precambrian Research, 150, 221-256.

Torsvik, T. H., Meert, J. G., 1995. Early Proterozoic palaeomagnetic data from the Pechenga Zone (north-west Russia) and their bearing on Early Proterozoic palaeogeography. Geophysical Journal International, 122, 520-536.

Torsvik, T. H., Carter, L. M., Ashwal, L. D., Bhushan, S. K., Pandit, M. K., Jamtveit, B., 2001. Rodinia refined or obscured: palaeomagnetism of the Malani igneous suite (NW India). Precambrian Research, 108, 319-333.

Torsvik, T.H., Smethurst, M.A., Meert, J.G., Van der Voo, R., McKerrow, W.S., Brasier, M.D., Sturt, B.A. and Walderhaug, H., 1996. Continental breakup and collision in the Neoproterozoic and Phanerozoic-A tale of Baltica and Laurentia. Earth Science Reviews, 40, 229-258.

Turner, C.C., Meert, J.G., Pandit, M.K., Kamenov, G.D., 2014. A detrital zircon U-Pb and Hf isotopic transect across the Son Valley sector of the Vindhyan basin, India: Implications for basin evolution and paleogeography. Gondwana Research, 26, 348-364.

Valet, J., Besse, J., Kumar, A., Vadakke-Chanat, S., Philippe, E., 2014. The intensity of the geomagnetic field from 2.4 Ga old Indian dykes. Geochemistry, Geophysics, Geosystems, 15, 2426-2437.

Van der Voo, R., 1990. The reliability of paleomagnetic data. Tectonophysics, 184, 1-9.

Veikkolainen, T., Pesonen, L.J., Evans, D.A.D., 2014. Paleomagia: A PHP/MYSQL database of the Precambrian paleomagnetic data, Studia Geophysica et Geodaetica, 58, 425-441.

Veikkolainen, T. and Pesonen, L.J., 2014. Paleosecular variation, field reversals and the stability of the geodynamo in the Precambrian. Geophysical Journal International, 199, 1515-1526.

Venkatesh, A. S., Rao, G. P., Rao, N. P., Bhalla, M.S., 1987. Palaeomagnetic and geochemical studies on dolerite dykes from Tamil Nadu, India. Precambrian Research, 34, 291-310.

Venkateshwarlu, M., Chalapathi-Rao, N.V., 2013. New paleomagnetic and rock magnetic results on Mesoproterozoic kimberlites from the Eastern Dharwar craton southern India: towards constraining India's position in Rodinia. Precambrian Research, 224, 588-596.

Venkateshwarlu, M., Khanna, T.C., 2015, Palaeomagnetic and Rock magnetic investigations on Gadwal "Dike 2", eastern Dharwar craton, India. Journal of the Indian Geophysical Union, 19, 447-453.

Vijaya Rao, V., Krishna, V.G., 2013. Evidence for the Neoproterozoic Phulad Suture Zone and Genesis of Malani Magmatism in the NW India from deep seismic images: implications for assembly and breakup of the Rodinia. Tectonophysics, 589, 172-185.

Wang, W., Cawood, P. A., Zhou, M. F., Pandit, M. K., Xia, X. P., & Zhao, J. H., 2017. Low-δ18O rhyolites from the Malani igneous suite: A positive test for South China and NW India linkage in Rodinia. Geophysical Research Letters, 44, 10-298.

Wang, W., Cawood, P.A., Pandit, M.K., Zhou, M.F., Zhao, J.H., 2019, Evolving passive-and active-margin tectonics of Paleoproterozoic Aravalli Basin, NW India: Geological Society of America Bulletin, 131,426-443.

Wingate, M.D., Evans, D.A.D., 2003. Paleomagnetic constraints on the Proterozoic tectonic evolution of Australia. Geological Society, Special Publication 206, 77–91.

Wingate,M.T.D., Pisarevsky,S.A., Gladkochub,D.P., Donskaya,T.V., Konstantinov,K.M., Mazukabzov,A.M., Stanevich,A.M., 2009. Geochronology and paleomagnetism of mafic igneous rocks in the Olenek Uplift, northern Siberia: implications for Mesoproterozoic supercontinents and paleogeography. Precambrian Research, 170, 256-266.

Wingate, M.T., Pisarevsky, S., de Waele, B., 2010. Paleomagnetism of the 765 Ma Luakela volcanics in Northwest Zambia and implications for Neoproterozoic positions of the Congo Craton. American Journal of Science, 310, 1333-1344.

Wu, H., 2005. New paleomagnetic results from Mesoproterozoic successions in Jixian area, North China Block, and their implications for paleocontinental reconstructions, Chinese University of Geosciences Beijing (dissertation).

Xu, H., Yang, Z., Peng, P., Meert, J.G., Zhu, R., 2014. Paleo-position of the North China craton within the supercontinent Columbia: constraints from new paleomagnetic results, Precambrian Research, 255, 276-293.

Zhao, G., Sun, M., Wilde, S.A., Li, S., 2004. A Paleo-Mesoproterozoic supercontinent: Assembly, growth and breakup, Earth-Science Reviews, 67, 91-123.

Zhao, G.C., Li, S.Z., Sun, M., Wilde, S.A., 2011. Assembly, accretion, and break-up of the Palaeo-Mesoproterozoic Columbia supercontinent: records in the North China Craton revisited. International Geology Review, 53, 1331–1356.

Figure Legends

Figure 1. (modified from Meert and Pandit, 2015) Simplified geological map of Peninsular India showing major Archean nuclei, Proterozoic basins and tectonized regions. Abbreviations as follows: **Basin Names**: MB=Marwar Basin; VB=Vindhyan Basin; ChB=Chhattisgarh Basin; CuB=Cuddapah Basin; KBB=Kaladgi-Bhima Basin; IB=Indravati Basin| **Tectonized Regions**: NSL=Narmada-Son Lineament; AFB=Aravalli Fold Belt; DFB=Delhi Fold Belt; CIS=Central Indian Suture; CITZ=Central Indian Tectonic Zone; SMB=Satpura Mobile Belt; CGC=Chottanagpur Gneissic Complex; EGMB=Eastern Ghats Mobile Belt; PCSZ=Palghat-Cauvery Shear Zone; KGB=Karimnagar Granulite Belt; BPG=Bhopalpatnam Granulite Belt; **Other Abbreviations**: CG=Closepet Granite; WDD=Western Dharwar Domain; EDD=Eastern Dharwar Domain; SIB=Southern Indian basement region (Dharwar, Bastar and Singhbhum cratons); NIB=Northern Indian basement regions (Aravalli-Banded Gneiss Complex and Bundelkhand craton); MR=Mahanadi Rift and PG=Prahnita-Godavari rift.

Figure 2: (a) Histogram of Q-values for paleomagnetic studies in India (203 studies); (b) Q-value distribution of pre-2000 studies from India and (c) Q-value distribution of post-2000 studies on Precambrian rocks in India. Light-shaded bars $Q \leq 3$. Dark-shaded bars $Q \geq 4$.

Figure 3: (modified after French and Heaman, 2010 and Söderlund et al., 2019) Geological map of the Dharwar Craton showing the locations of major dyke swarms and ultramafic intrusions and basins.

Figure 4: (modified after Meert and Pandit, 2015). Geological map of the Bastar Craton showing the location of major dyke swarms and basins.

Figure 5: (modified from Kumar et al., 2017). Geological map of the Singhbhum Craton showing the locations of major dyke swarms and basins.

Figure 6: (modified from Pradhan et al., 2010). Geological map of the Bundelkhand Craton showing locations of dykes, ultramafic intrusions and basins.

Figure 7: Individual virtual geomagnetic poles (VGP's) and associated a95 envelopes, mean paleomagnetic pole (A95) for (a) ~2367 Ma dykes in the Dharwar Craton and northern segment of the Southern Granulite Terrane along (b) for ~2252 Ma dykes in the Dharwar Craton (c) for ~2216 Ma dykes in the Dharwar Craton and northern segment of the southern granulite terrane (d) for ~2207 Ma dykes in the Dharwar Craton and northern segment of the southern granulite (e) for ~1980 Ma dykes in the Bundelkhand Craton. All mean results are listed in Table 1.

Figure 8: Individual virtual geomagnetic poles (VGP's) and associated a95 envelopes, mean paleomagnetic pole (A95) for (a) ~1890 Ma dykes in the Dharwar and Bastar cratons and northern segment of the Southern Granulite Terrane (b) for ~1765 Ma dykes in the Singhbhum Craton (c) for ~1465 Ma dykes in the Bastar Craton. All mean results are listed in Table 1.

Figure 9: Individual virtual geomagnetic poles (VGP's) and associated a95 envelopes, mean paleomagnetic pole (A95) for (a) ~1075 Ma dykes, kimberlites and Upper Vindhyan sedimentary rocks from the Bundelkhand Craton and kimberlites from the Dharwar craton. (b) for ~750-771 Ma Malani Igneous Suite in Rajasthan. All mean results are listed in Table 1.

Figure 10: (a) Model G fits to paleomagnetic data from the Indian cratonic nuclei; (b) paleolatitudinal plot of India and (c) Igneous barcode for the SIB and NIB of India. Arrow (a) designates the assembly of Bastar, Southern Granulite terrane and Dharwar cratons based on paleomagnetic and geochronological data. Arrow (b) is the proposed amalgamation of the SIB according to Soderlund et al. (2019). Unshaded is a proposed 2250 or 2216 Ma dyke swarm in the Bastar craton identified by preliminary paleomagnetic directions. Arrow (c) shows our preferred age for SIB amalgamation sans confirmation of (b) dykes. Arrow (d) shows the timing of Peninsular India assembly between 1.1-10 Ga.

Figure 11: (a) Indian cratonic coherence at 2.367 Ga; (b) at 1.765 Ga and (c) Peninsular India at 1.1-1.0 Ga.

Figure 12: Paleomagnetic poles from Table 1.

Figure 13: Pre-Columbia (a) 2.4 Ga schematic of Bastar/Dharwar, the Yilgarn craton (western Australia) and the Kaapvaal craton (southern Africa); (b) 2.22 Ga schematic of Bastar/Dharwar, Kaapvaal, Superior and Slave cratons; (c) 2.08 Ga schematic of the Dharwar/Bastar, Kaapvaal, Superior, Greenland, Guiana and Fennoscandian cratons. Rotation parameters and poles are listed in Table 2. NP=North Geographic pole.

Figure 14: Columbia/Nuna (a) 1.88 Ga schematic of Dharwar/Bastar, Amazonia, Kaapvaal, Superior, Slave, Wyoming, Fennoscandian and Siberian cratons; (b) 1.77 Ga schematic featuring united south Indian Blocks (SIB), Fennoscandia and Sarmatia, Amazonia, North China and Laurentia; (c) 1.45 Ga reconstruction with South Indian Blocks, Australian blocks, Siberia, Congo-Sao Francisco, Baltica, Siberia and North China. South Indian blocks are also shown using the opposite hemisphere option near the Congo-Sao Francisco craton. Rotation parameters and poles are listed in Table 2. NP=North Geographic pole.

Figure 15: (a) Comparison between the 1.1-1.0 Ga paleolatitudinal position of India in Rodinia according to Li et al. (2008) and 1.073 Ga position according to the data given in Table 1.Rotation parameters: India-1100 Ma (Li et al., 2008) 50.47° N, 151.38° E, -97.38°; India 1050 Ma (Li et al., 2008) 55.77° N, 122.85° E, -71.67°; India 1000 Ma (Li et al., 2008) 17° N, 100.29° E, -58.15°;1073 Ma (this study) 0° N, 126° E, -132.6° (b) Comparison of the 0.77 Ga position of India expected in the traditional Gondwana fit based on paleomagnetic data from Australia (India-A); India-B is the latitudinal position of India relative to Australia based on data in Table 1 (Euler Rotations: India-A 42.7° N, 153.8° E, +38.9°; East Antarctica 1.63° N, 222.8° E, −75.2°; India-B 0° N, 345.7° E, +20.6°; India-C 0° N, 345.7° E, −159.4) and India-C representing a closest-Australia approach of India based on the Malani (0.77 Ga) pole.

Simplified Regional Geology of Peninsular India

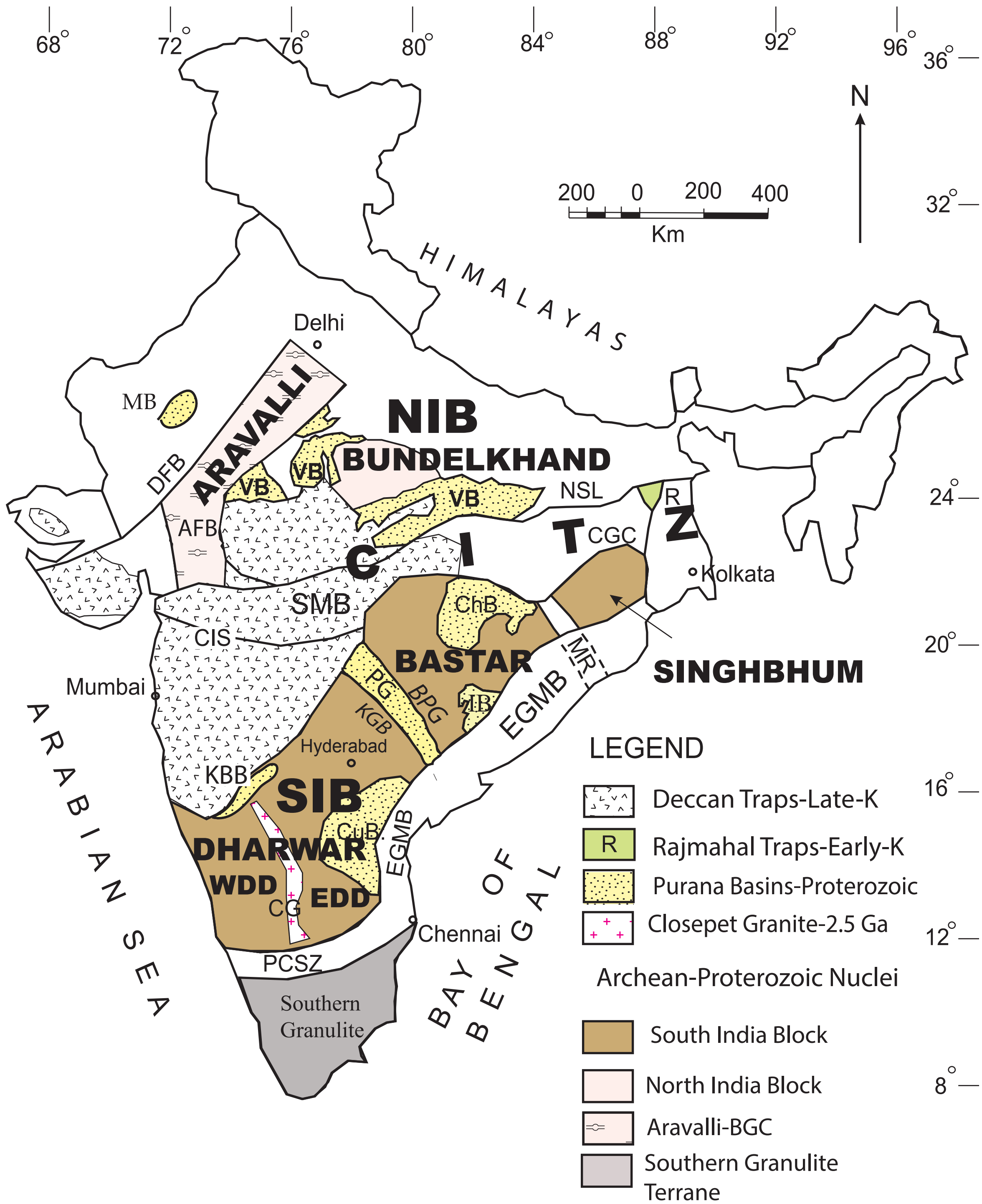

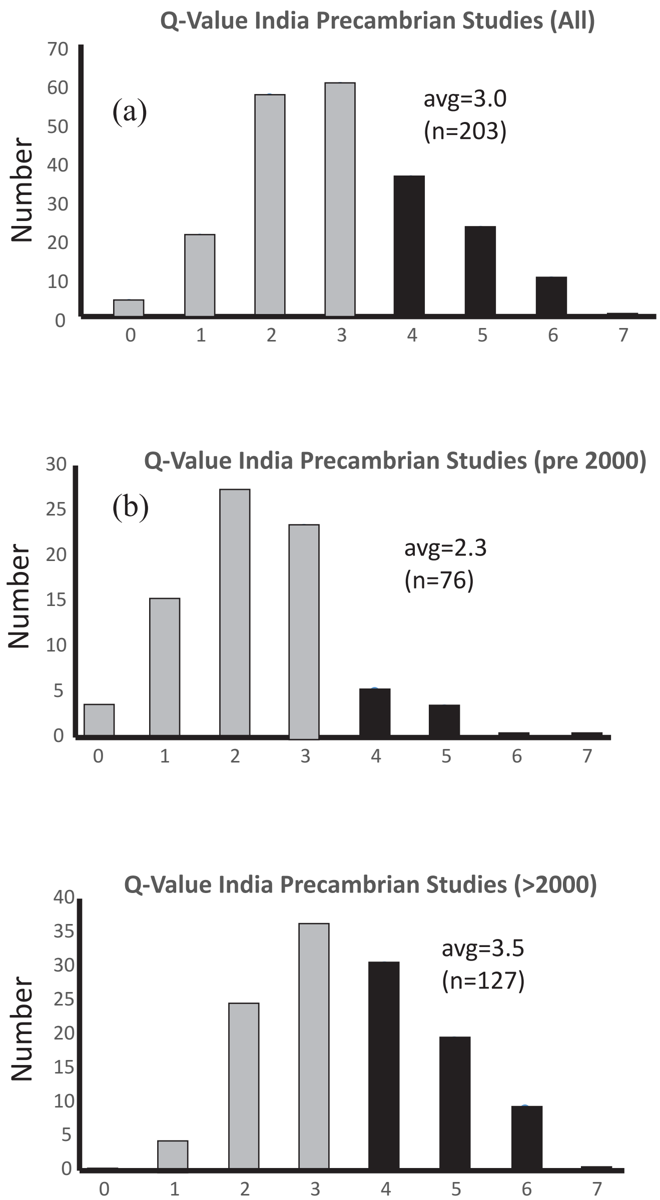
Q-Value India Precambrian Studies (All)
(a)
avg=3.0
(n=203)
Number
70
60
50
40
30
20
10
0
0
1
2
3
4
5
6
7
Q-Value India Precambrian Studies (pre 2000)
(b)
avg=2.3
(n=76)
Number
30
25
20
15
10
5
0
0
1
2
3
4
5
6
7
Q-Value India Precambrian Studies (>2000)
avg=3.5
(n=127)
Number
40
35
30
25
20
15
10
5
0
0
1
2
3
4
5
6
7

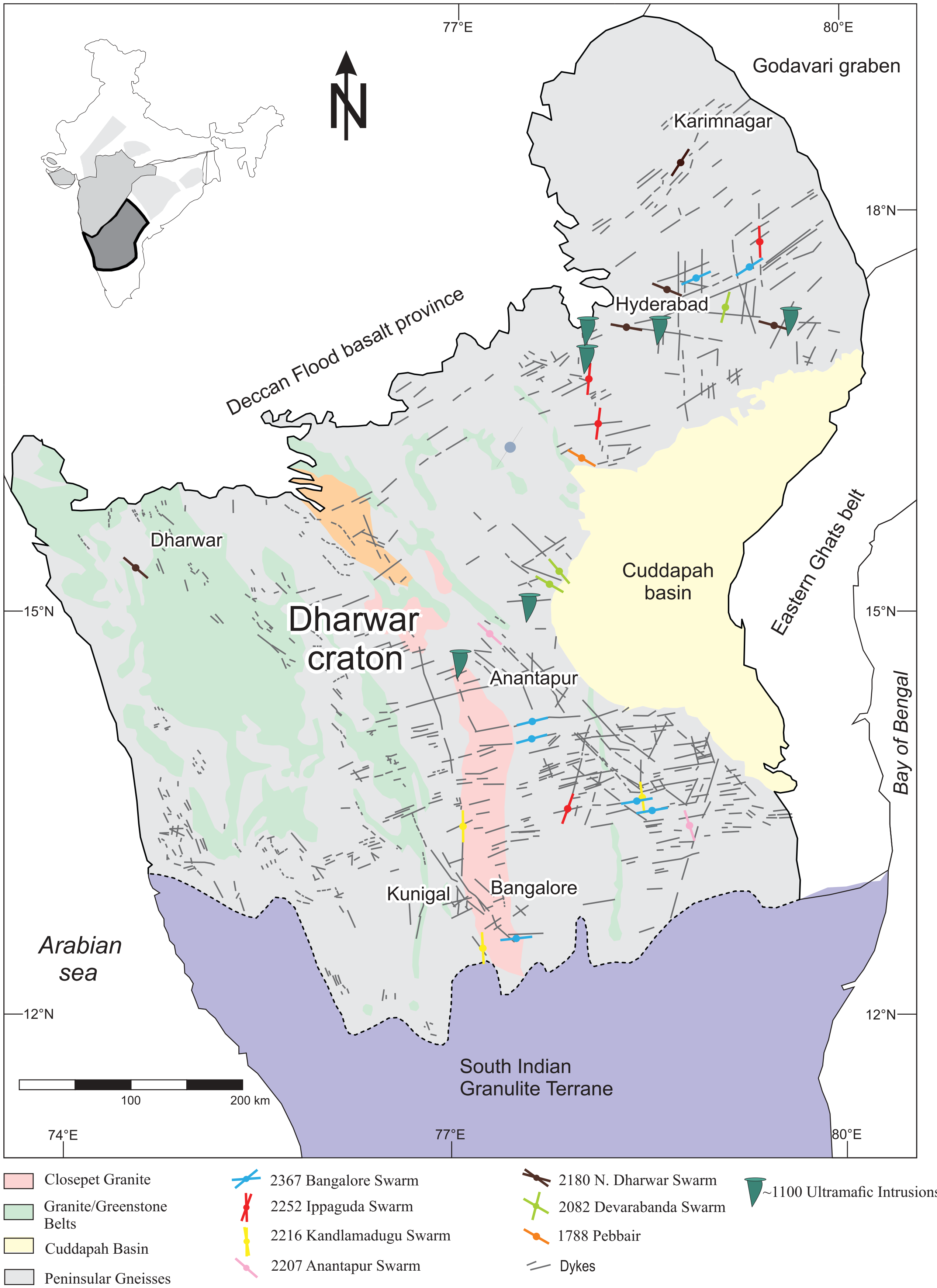
77°E
80°E
Godavari graben
Karimnagar
18°N
Hyderabad
Deccan Flood basalt province
Dharwar
Dharwar craton
Cuddapah basin
Eastern Ghats belt
15°N
Anantapur
Bay of Bengal
Kunigal
Bangalore
Arabian sea
12°N
South Indian Granulite Terrane
100
200 km
74°E
77°E
80°E
Closepet Granite
Granite/Greenstone Belts
Cuddapah Basin
Peninsular Gneisses
2367 Bangalore Swarm
2252 Ippaguda Swarm
2216 Kandlamadugu Swarm
2207 Anantapur Swarm
2180 N. Dharwar Swarm
2082 Devarabanda Swarm
1788 Pebbair
Dykes
~1100 Ultramafic Intrusions

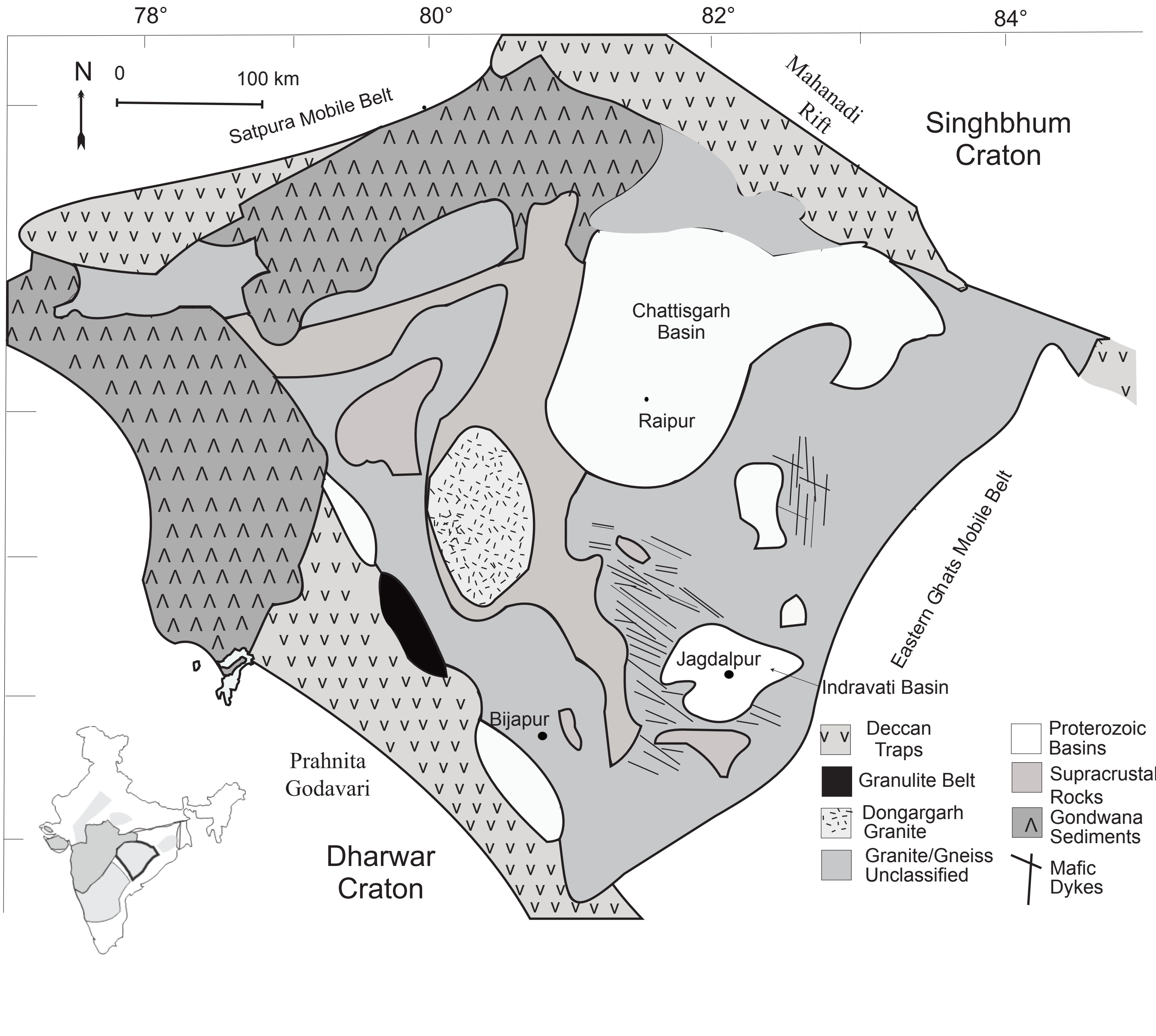
78°
80°
82°
84°
23°
21°
19°
N
0
100 km
Satpura Mobile Belt
Mahanadi Rift
Singhbhum Craton
Chattisgarh Basin
Raipur
Eastern Ghats Mobile Belt
Jagdalpur
Indravati Basin
Bijapur
Prahnita Godavari
Dharwar Craton
Deccan Traps
Granulite Belt
Dongargarh Granite
Granite/Gneiss Unclassified
Proterozoic Basins
Supracrustal Rocks
Gondwana Sediments
Mafic Dykes

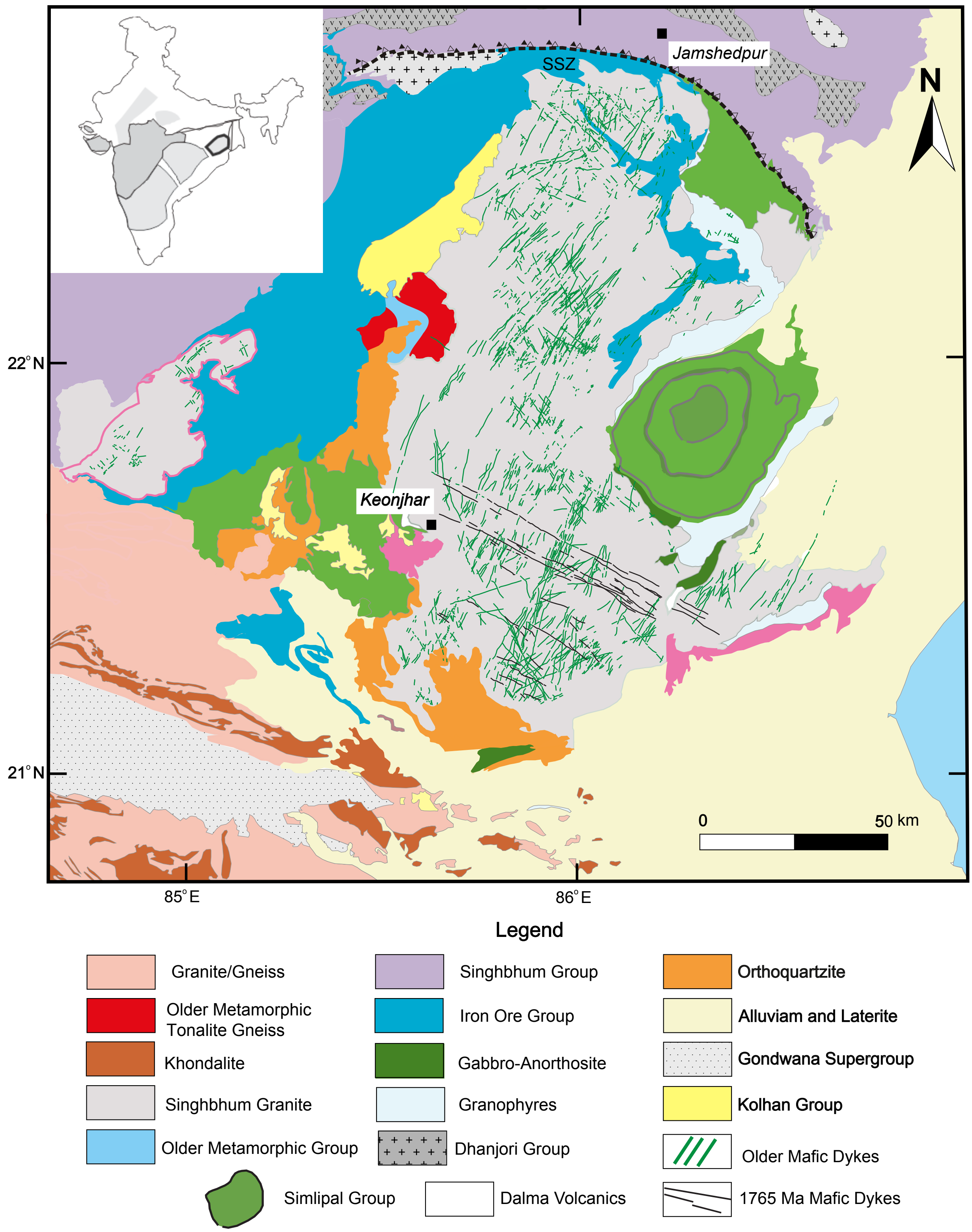

Jamshedpur
SSZ
N
22° N
21° N
Keonjhar
0
50 km
85° E
86° E
Legend
Granite/Gneiss
Older Metamorphic Tonalite Gneiss
Khondalite
Singhbhum Granite
Older Metamorphic Group
Singhbhum Group
Iron Ore Group
Gabbro-Anorthosite
Granophyres
Dhanjori Group
Orthoquartzite
Alluviam and Laterite
Gondwana Supergroup
Kolhan Group
Older Mafic Dykes
Simlipal Group
Dalma Volcanics
1765 Ma Mafic Dykes

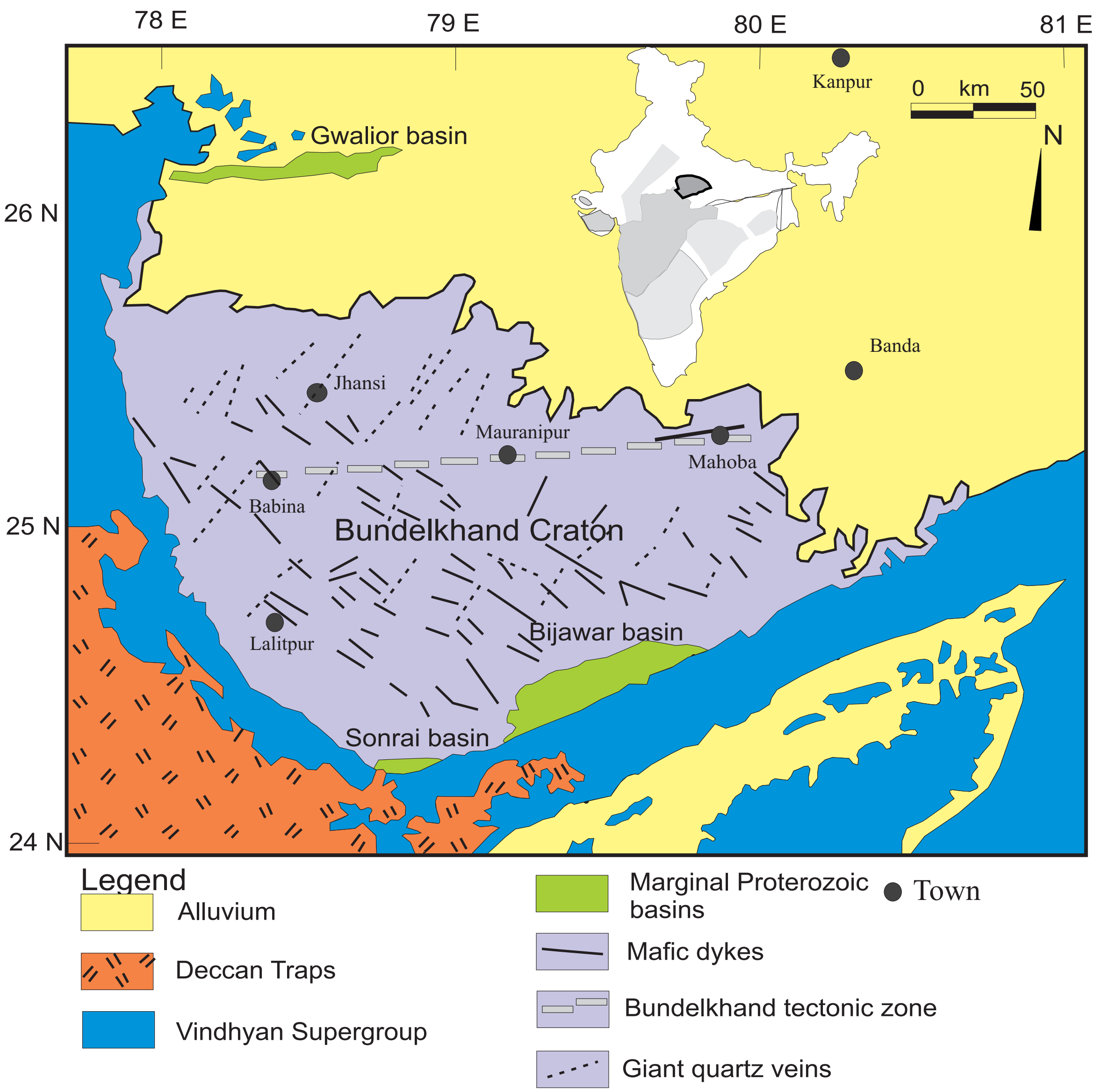
78 E
79 E
80 E
81 E
26 N
25 N
24 N
Kanpur
0 km 50
N
Gwalior basin
Banda
Jhansi
Mauranipur
Mahoba
Babina
Bundelkhand Craton
Lalitpur
Bijawar basin
Sonrai basin
Legend
Alluvium
Deccan Traps
Vindhyan Supergroup
Marginal Proterozoic basins
Town
Mafic dykes
Bundelkhand tectonic zone
Giant quartz veins

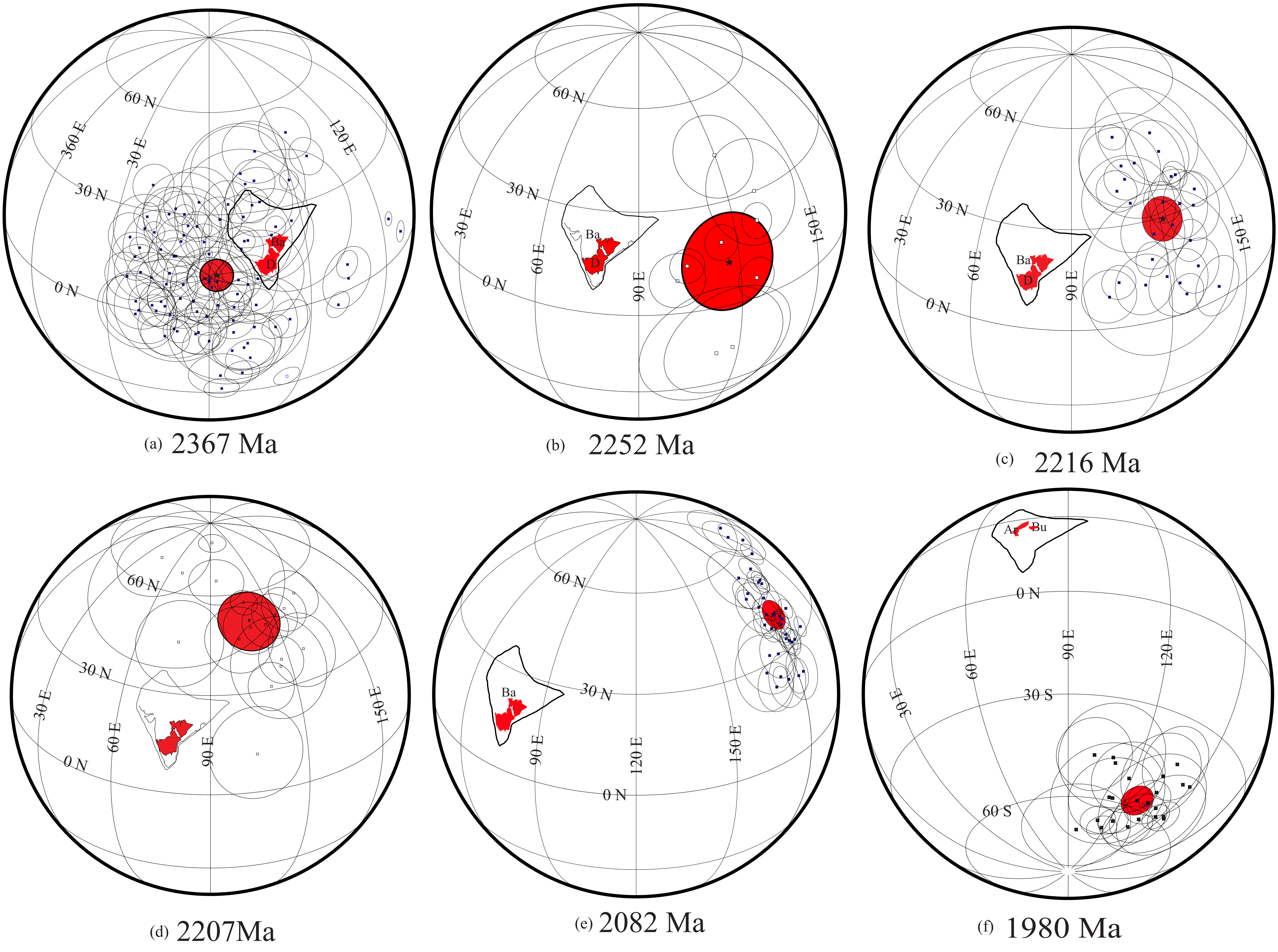
60 N
30 N
0 N
360 E
30 E
120 E
Ba
D
(a) 2367 Ma
60 N
30 N
0 N
30 E
60 E
90 E
150 E
Ba
D
(b) 2252 Ma
60 N
30 N
0 N
30 E
60 E
90 E
150 E
Ba
D
(c) 2216 Ma
60 N
30 N
0 N
30 E
60 E
90 E
150 E
(d) 2207Ma
60 N
30 N
0 N
90 E
120 E
150 E
Ba
(e) 2082 Ma
Ar
Bu
0 N
30 S
60 S
30 E
60 E
90 E
120 E
(f) 1980 Ma

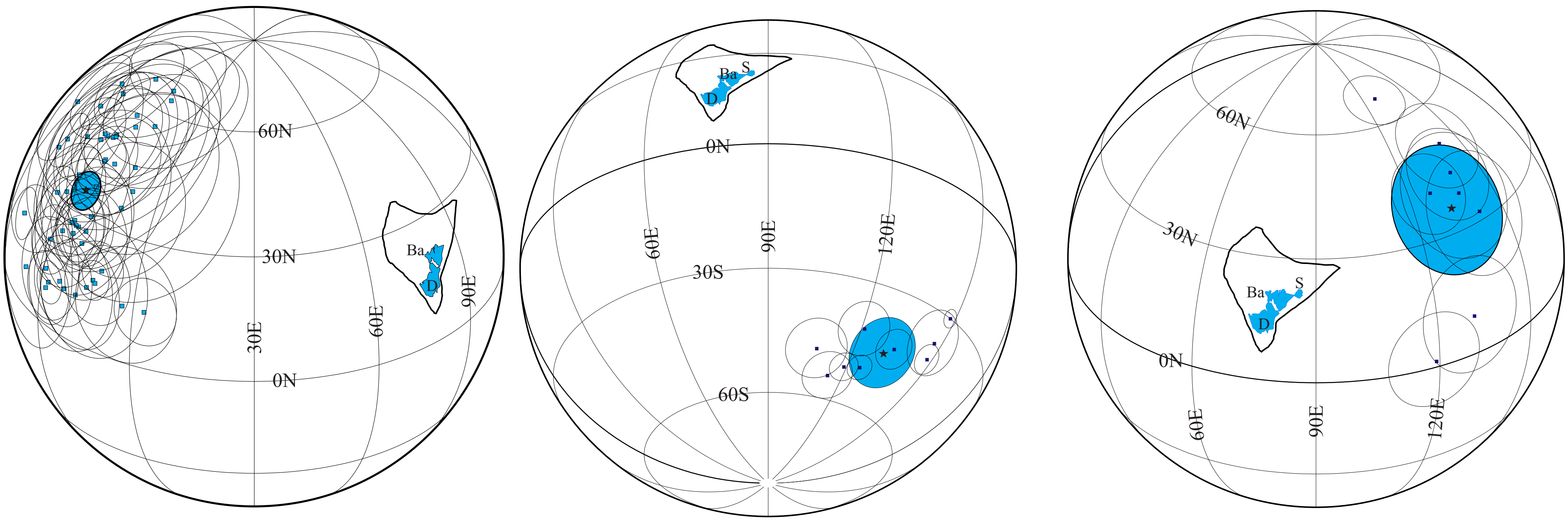

(a) 1888 Ma (b) 1765 Ma (c) 1465 Ma

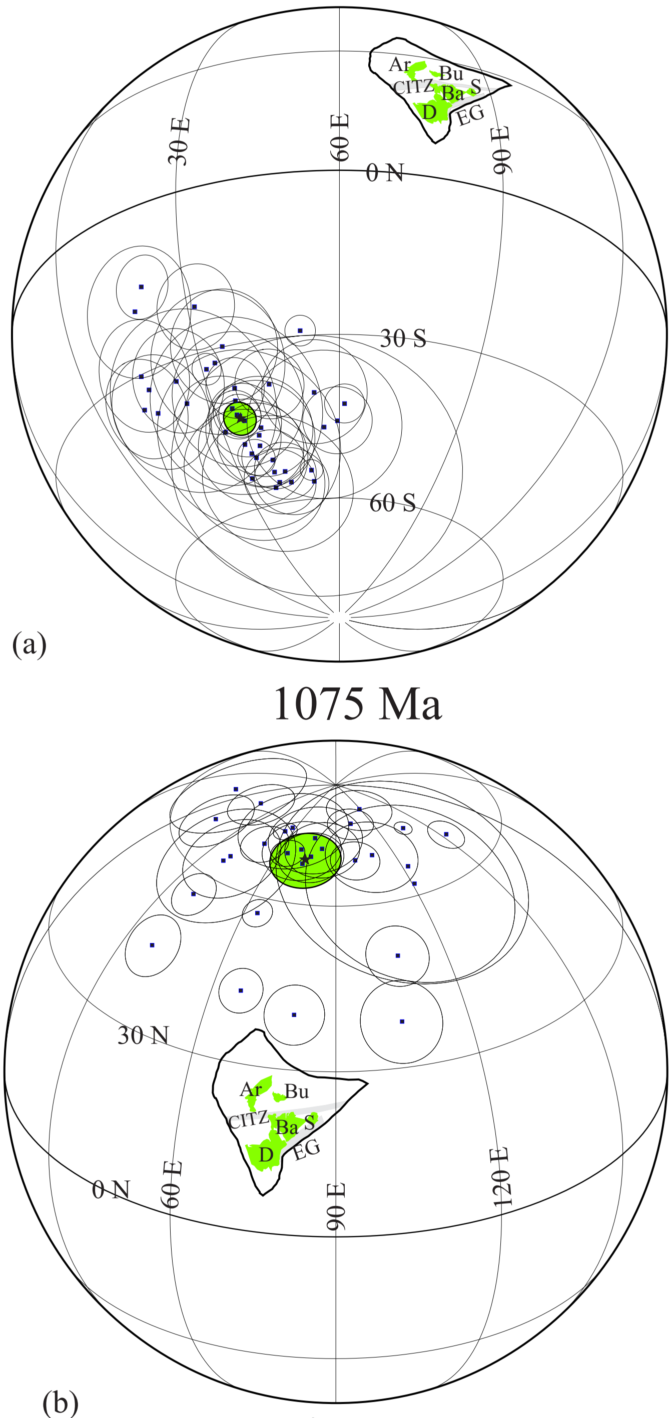

1075 Ma

770 Ma

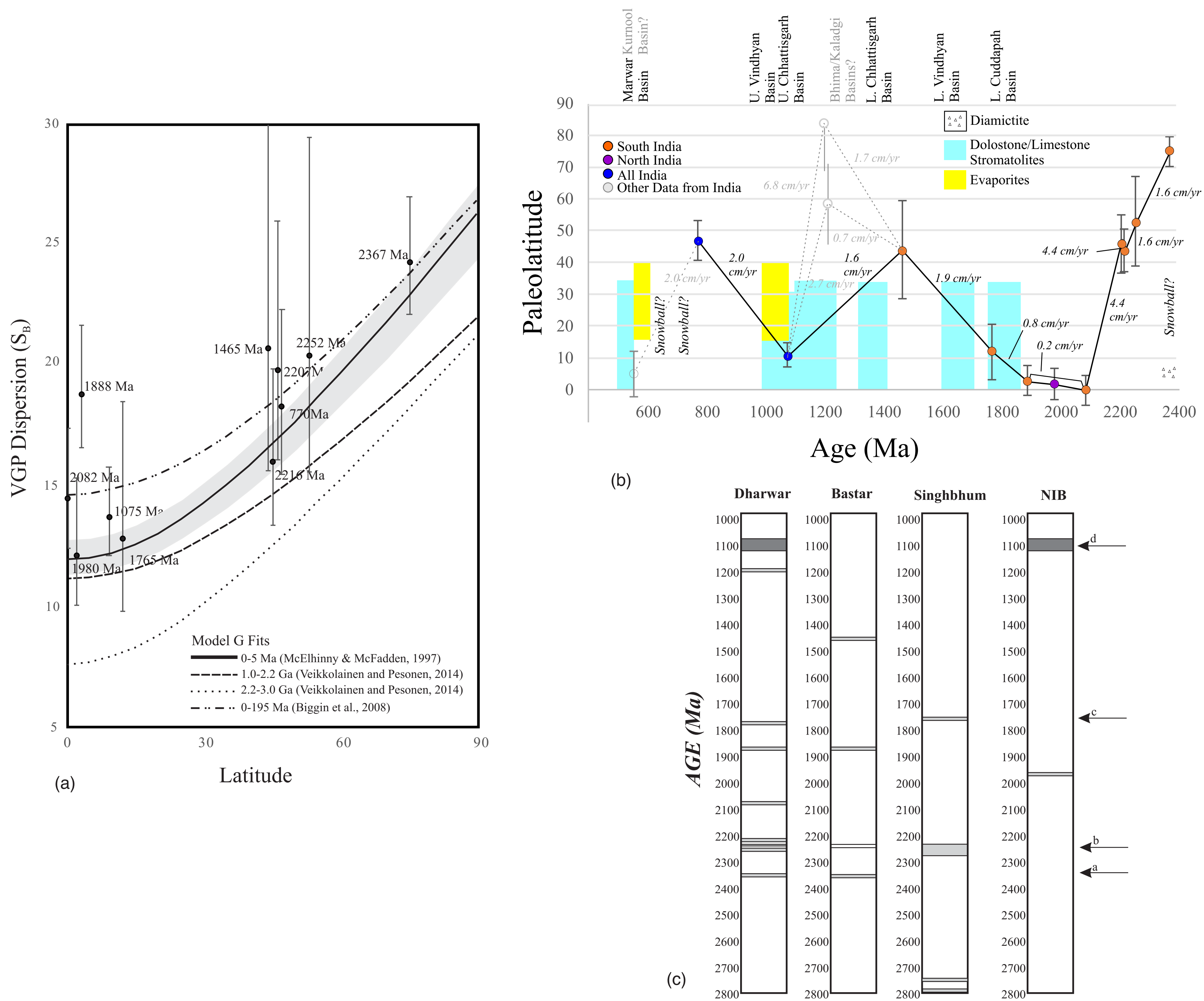

VGP Dispersion (S_B)
Latitude
1888 Ma
2082 Ma
1075 Ma
1980 Ma
1765 Ma
1465 Ma
2207 Ma
2252 Ma
770Ma
2216 Ma
2367 Ma
Model G Fits
0-5 Ma (McElhinny & McFadden, 1997)
1.0-2.2 Ga (Veikkolainen and Pesonen, 2014)
2.2-3.0 Ga (Veikkolainen and Pesonen, 2014)
0-195 Ma (Biggin et al., 2008)
(a)
Marwar Basin
Kurnool Basin?
U. Vindhyan Basin
U. Chhattisgarh Basin
Bhima/Kaladgi Basins?
L. Chhattisgarh Basin
L. Vindhyan Basin
L. Cuddapah Basin
Paleolatitude
Age (Ma)
South India
North India
All India
Other Data from India
Diamictite
Dolostone/Limestone Stromatolites
Evaporites
Snowball?
2.0 cm/yr
1.6 cm/yr
1.9 cm/yr
0.8 cm/yr
0.2 cm/yr
4.4 cm/yr
1.6 cm/yr
1.7 cm/yr
6.8 cm/yr
0.7 cm/yr
2.7 cm/yr
(b)
Dharwar
Bastar
Singhbhum
NIB
AGE (Ma)
a
b
c
d
(c)

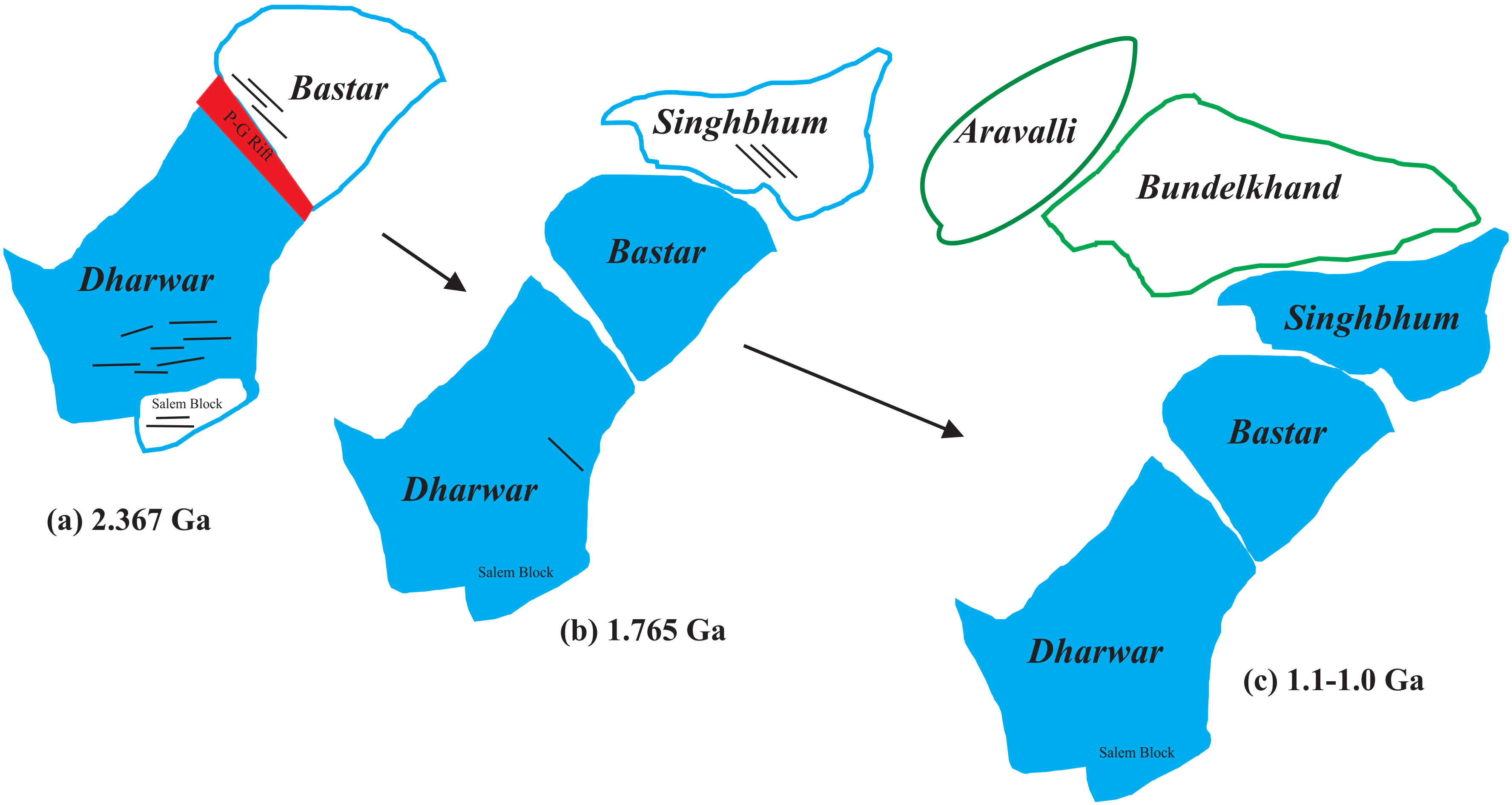

Bastar
P-G Rift
Dharwar
Salem Block
(a) 2.367 Ga
Singhbhum
Bastar
Dharwar
Salem Block
(b) 1.765 Ga
Aravalli
Bundelkhand
Singhbhum
Bastar
Dharwar
Salem Block
(c) 1.1-1.0 Ga

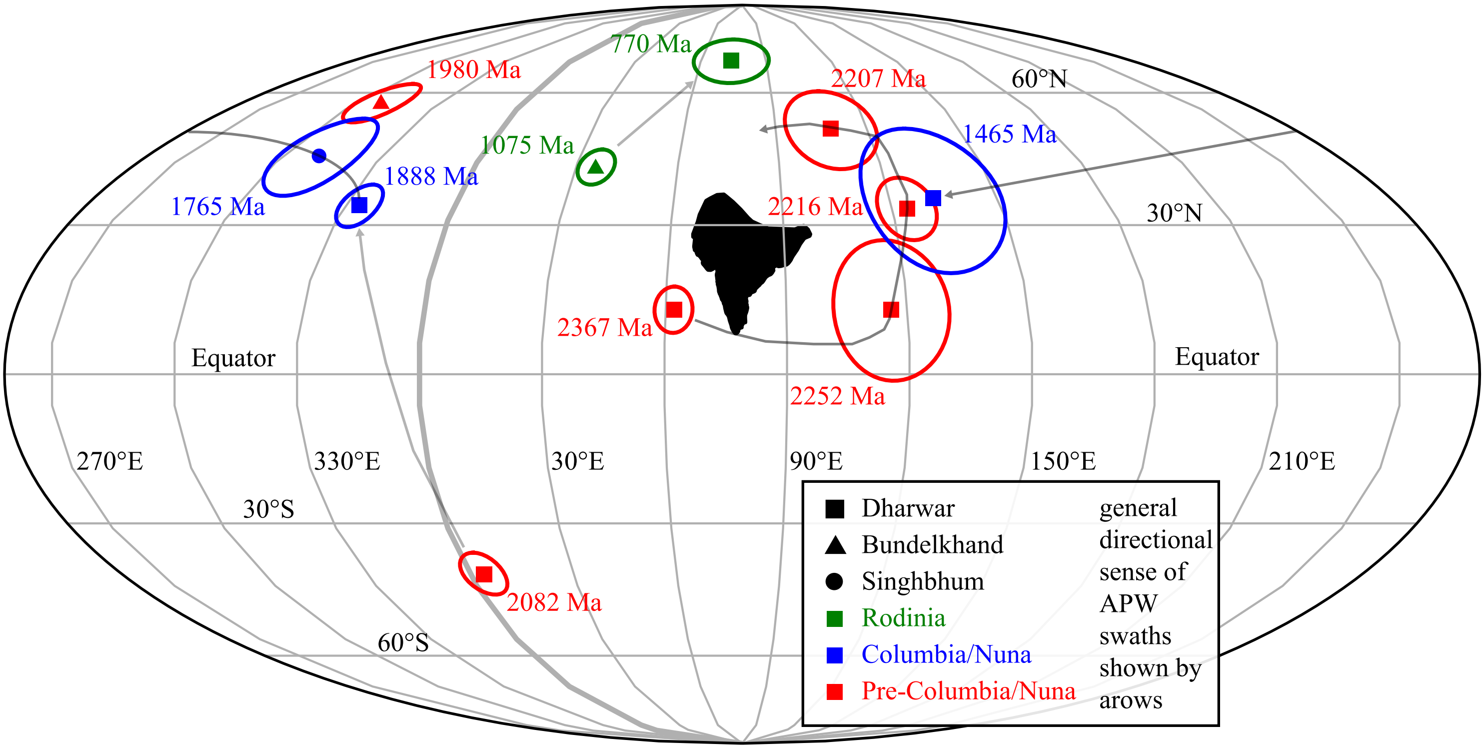
770 Ma
1980 Ma
2207 Ma
60°N
1075 Ma
1465 Ma
1888 Ma
1765 Ma
2216 Ma
30°N
2367 Ma
Equator
Equator
2252 Ma
270°E
330°E
30°E
90°E
150°E
210°E
30°S
2082 Ma
60°S
Dharwar
Bundelkhand
Singhbhum
Rodinia
Columbia/Nuna
Pre-Columbia/Nuna
general directional sense of APW swaths shown by arows

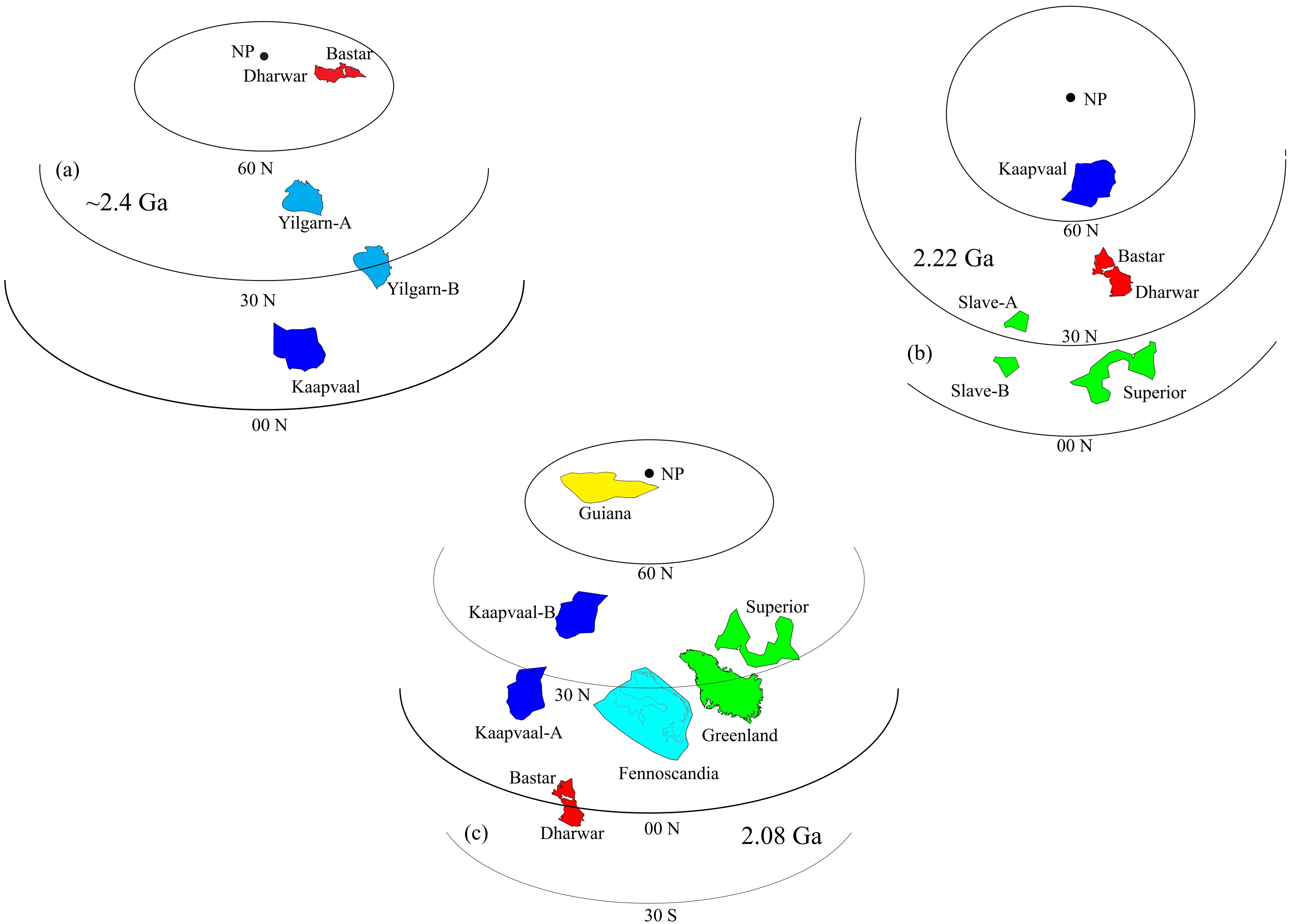
NP
Bastar
Dharwar
(a)
60 N
~2.4 Ga
Yilgarn-A
Yilgarn-B
30 N
Kaapvaal
00 N
NP
Kaapvaal
60 N
2.22 Ga
Bastar
Dharwar
Slave-A
30 N
(b)
Slave-B
Superior
00 N
NP
Guiana
60 N
Kaapvaal-B
Superior
30 N
Kaapvaal-A
Greenland
Fennoscandia
Bastar
(c)
Dharwar
00 N
2.08 Ga
30 S

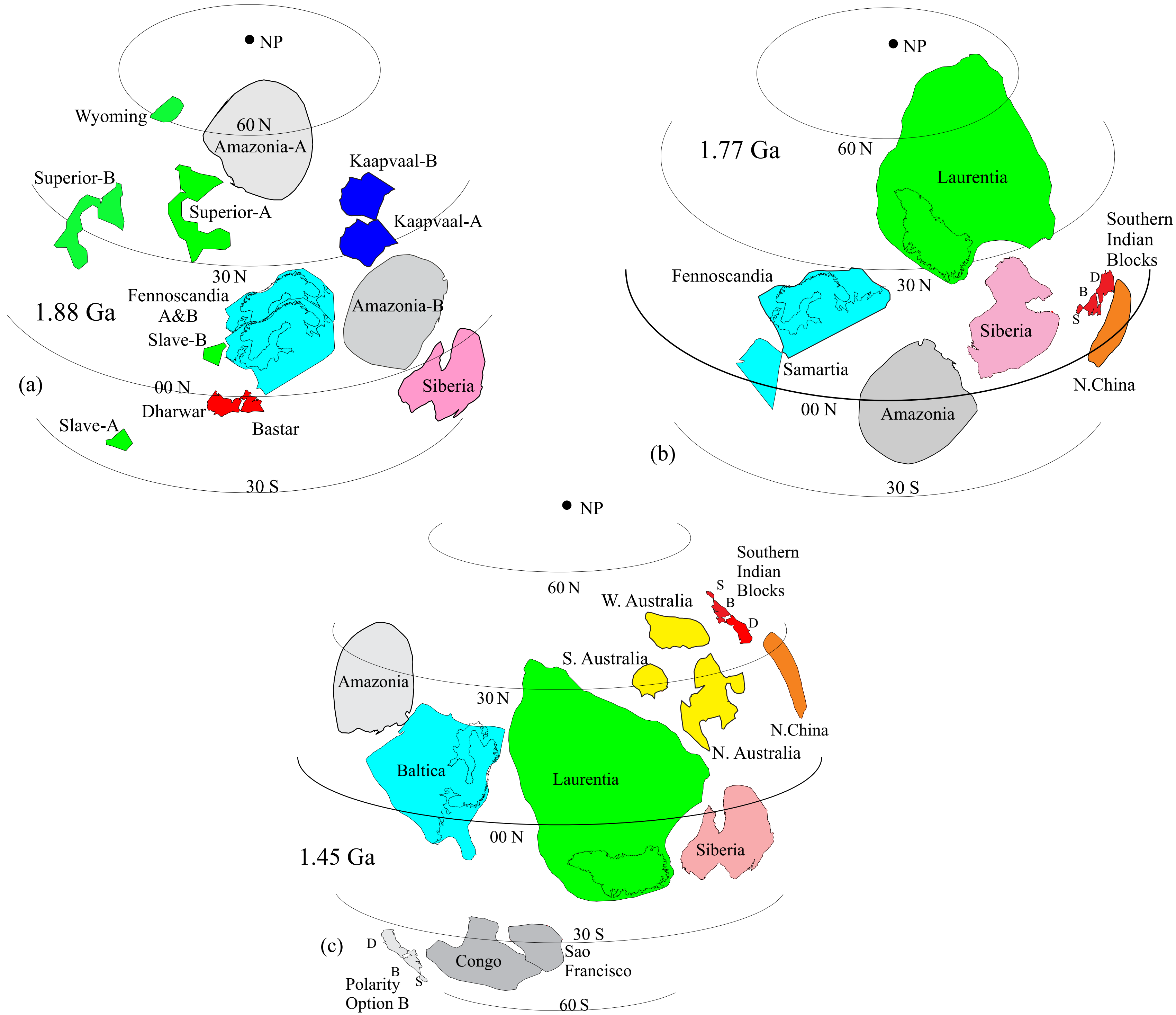
NP
Wyoming
60 N
Amazonia-A
Superior-B
Superior-A
Kaapvaal-B
Kaapvaal-A
30 N
Fennoscandia
A&B
1.88 Ga
Amazonia-B
Slave-B
(a)
00 N
Siberia
Dharwar
Slave-A
Bastar
30 S
NP
1.77 Ga
60 N
Laurentia
Southern
Indian
Blocks
Fennoscandia
30 N
D
B
S
Siberia
Samartia
N.China
00 N
Amazonia
(b)
30 S
NP
Southern
Indian
Blocks
60 N
W. Australia
S
B
D
S. Australia
Amazonia
30 N
N.China
Baltica
N. Australia
Laurentia
00 N
Siberia
1.45 Ga
30 S
Sao
Francisco
(c)
D
Congo
B
S
Polarity
Option B
60 S

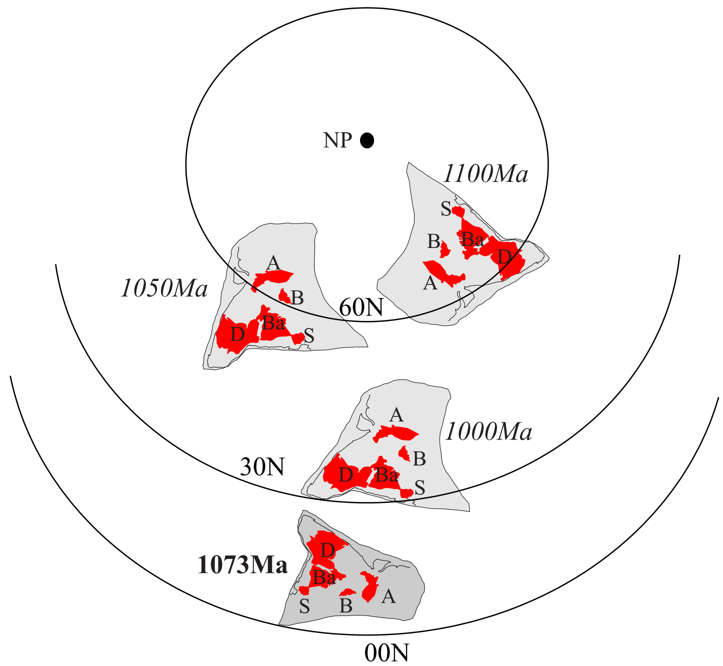
NP
1100Ma
S
B
Ba
D
A
A
1050Ma
B
60N
D
Ba
S
A
1000Ma
B
30N
D
Ba
S
D
1073Ma
Ba
S
B
A
00N

(a)

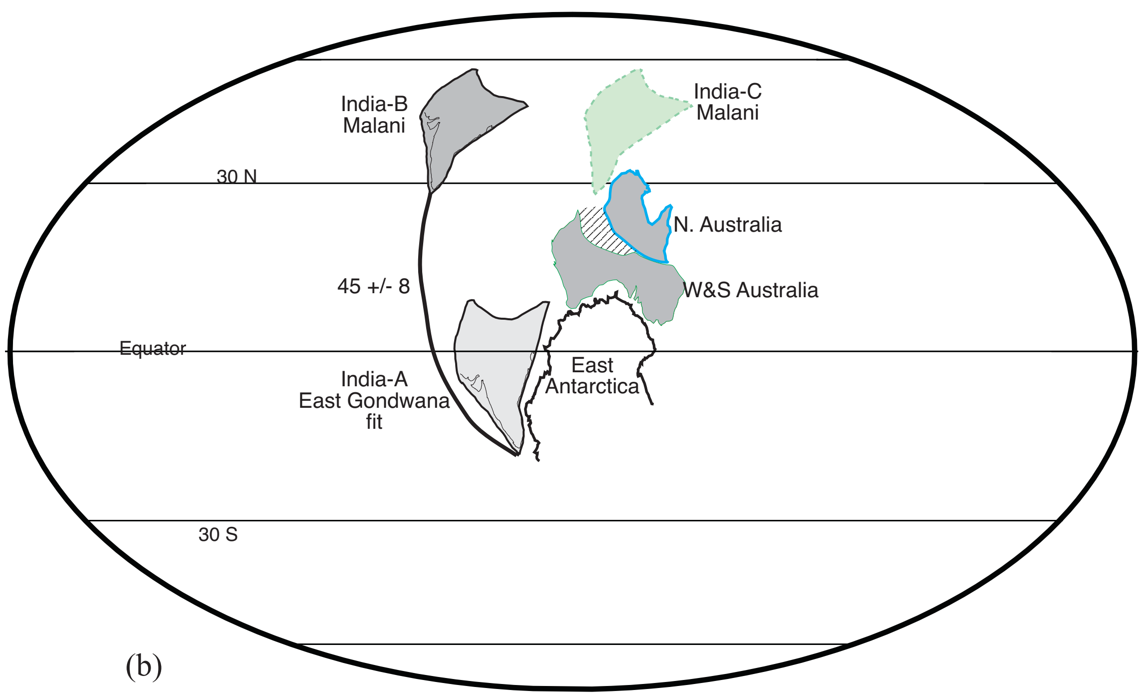
India-B
Malani
India-C
Malani
30 N
N. Australia
45 +/- 8
W&S Australia
Equator
East
Antarctica
India-A
East Gondwana
fit
30 S

(b)

Table 1. Key Paleomagnetic Poles from Peninsular India

Pole	Age	N/n	Slat	Slong	Plat	Plong	K	A95	S_B	%R	λ_s	$A95_{min}$	$A95_{max}$	Q
Dharwar-Bastar-SGT[1]	2367 Ma	93/791	15° N	77.5° E	12.8° N	62° E	11	4.6°	24.3°	93%	75°	1.9°	4.7°	6
Dharwar-Bastar Craton[2]	2252 Ma	9/64	14.8° N	77.5° E	12.8° N	116° E	14	14°	20.4°	88%	53°	5°	20.5°	4
Dharwar-Bastar Craton[3]	2216 Ma	21/156	14.8° N	76.8° E	33.5° N	124° E	25	6.6°	16.0°	90%	45°	3.6°	12.0°	5
Dharwar-Bastar Craton[4]	2207 Ma	17/140	14.8° N	76.8° E	51.2° N	108° E	16	9.2°	19.8°	0%	46°	3.9°	13.8°	5
Dharwar-Bastar Craton[5]	2082 Ma	34/392	16.5° N	79° E	40.5° N	184° E	31	4.5°	14.5°	0%	0°	2.9°	8.9°	6
Bundelkhand Craton[6]	1980 Ma	22/263	25° N	80° E	57.5° N	309° E	43	4.8°	12.1°	86%	2°	3.5°	11.7°	6
Dharwar-Bastar Craton[7]	1888 Ma	54/434	15.7° N	79° E	35.0° N	334° E	18	4.6°	18.8°	81%	3°	2.4°	6.4°	6
South India[8]	1765 Ma	9/86	21.5° N	86° E	44.9° N	311° E	36	8.7°	12.8°	100%	12°	5.0°	20.5°	6
South India[9]	1465 Ma	8/60	20.8° N	82.6° E	35.7° N	132° E	14	15.5°	20.7°	13%	44°	5.2°	22°	5
India[10]	1075 Ma	56/500	27° N	77.5° E	44.4° N	215° E	34	3.3°	13.7°	61%	9°	2.4°	6.5°	5
India[11]	770 Ma	28/207	26° N	73° E	69.4° N	75° E	19	6.4°	18.3°	4%	47°	3.2°	10°	7

Notes: N=Number of sites; n=number of samples; Slat=Site Latitude; Slong=Site Longitude; Plat=Pole Latitude; Plong=Pole Longitude; K=Fisher (1953) precision parameter for mean pole; A95=circle of 95% confidence calculated from VGP directions;%R=percentage of normal polarity (-inclinations taken as reverse) S_B= VGP scatter (McElhinny and McFadden, 1997); λ_s=paleolatitude for site; $A95_{min}$=Deenan et al.(2011) minimum; $A95_{max}$=Deenan et al. (2011) maximum; Q=Van der Voo (1990) criteria. References [1]Dawson and Hargraves (1994); Halls et al. (2007); Piispa et al. (2011); Belica et al. (2014); Venkatash et al. (1987); Radhakrishna and Joseph (1996);Kumar and Bhalla (1983); Bhalla et al. (1983); Hasnain and Qureshy (1971); Kumar et al. (2012a); Radhakrishna et al. (2013); Dash et al. (2013); Pivarunas et al. (2019); Babu et al. (2018); Valet et al. (2014):[2]Belica et al. (2014); Radhakrishna et al. (2013b); Kumar et al. (2012a) compiled by Nagaraju et al. (2018a), recalculated from original 2252 Ma pole reported in paper at 16° N, 119° E (a95=9°); [3]Nagaraju et al. (2018a) ;Kumar et al. (2012a,b); Belica et al. (2014); Piispa et al. (2011):[4]Nagaraju et al. (2018a); Belica et al. (2014); Radhakrishna et al. (2013b): [5]Kumar et al. (2015); Belica et al. (2014); Piispa et al. (2011); Radhakrishna et al. (2013a): [6]Pradhan et al. (2012); Radhakrishna et al. (2013b):[7]Clark (1982); Belica et al. (2014); Meert et al. (2011); Hargraves and Bhalla (1983); Kumar and Bhalla (1983); Bhalla et al. (1980); Prasad et al. (1987):[8]Shankar et al. (2018):[9]Pisarevsky et al. (2013):[10]Venkateshwarlu et al. (2013); Pradhan et al (2012);Malone et al. (2008); Gregory et al. (2006);Miller and Hargraves (1994); McElhinny et al. (1978); Klootwijk (1973) :[11]Klootwijk (1975); Torsvik et al. (2001); Gregory et al. (2009).

Table 2. Paleomagnetic Poles used in Reconstructions

Pole Name	Age	Plat	Plong	A95	Q	Reference
~2367 Ma[1]						
Dharwar-Bastar Swarm-S. India	2367 Ma	13° N	62° E	4.6°	6	(see references table 1)
Widgiemooltha-Yilgarn-A	2415 Ma	10° N	339° E	4.8°	7	Smirnov et al., 2013
Eraynia Dykes- Yilgarn-B	2401 Ma	23° S	330° E	11.4°	4	Pisarevsky et al., 2014
Ongeluk Lavas-Kaapvaal	2426 Ma	4° N	283° E	4.1°	6	Gumsley et al., 2017
2216 Ma[2]						
Dharwar craton dykes-S. India	2216 Ma	34° N	124° E	6.6°	5	(see references table 1)
Senneterre-Nippising-Superior	2216 Ma	16° N	278° E	---	7	Buchan et al., 1993; Buchan et al., 2000
Malley Dykes-Slave-A	2231 Ma	51° N	130° E	5.8°	5	Buchan et al., 2012
Dogrib Dykes-Slave-B	2193 Ma	31° N	135° E	7°	6	Mitchell et al., 2014
Hekpoort- Kaapvaal	2225 Ma	44° N	220° E	8.0°	6	Humbert et al., 2017
2080 Ma[3]						
Dharwar Dykes-S. India	2082 Ma	41° N	184° E	4.5°	6	(see references table 1)
Waterberg UBS-I-Kaapvaal-A	2054 Ma	37° N	51° E	10.9°	5	de Kock et al., 2006
Mean Guiana Shield	2093 Ma	2 S	113 E	12	4	Théveniaut et al., 2006
Bushveld Complex-Kaapvaal-B	2049 Ma	19° N	31° E	3.9°	6	Letts et al., 2009
Lac Esprit/Cauchon Lake/Ft. Frances-Superior	2079 Ma	55° N	180° E	12.5°	5	Evans and Halls, 2010
Kangamlut dykes-Greenland	2042 Ma	17° N	274° E	2.7°	4	Fahrig and Bridgwater, 1976
Kuetsyarvi-Fennoscandia	2058 Ma	25° N	301° E	19.9°	5	Torsvik and Meert, 1995
1888 Ma[4]						
Dharwar-Bastar-S. India	1888 Ma	34° N	334° E	4.5°	6	(see references table 1)
Ghost Dykes-Slave-A	1887 Ma	2.0° N	106° E	5°	6	Buchan et al., 2016
Slave B Mean	1876 Ma	-14° N	258° E	8.8°	6	Mitchell et al., 2010;Irving & McGlynn, 1979
Molson B+C2 Dykes-Superior-A	1879 Ma	29° N	218° E	4°	7	Evans and Halls, 2010
Haigh-Flaherty-Sot Mean-Superior-B	1870 Ma	1.0 N	246 E	3.9	7	Luleå Working Group, 2009
Mashonland dykes-Kaapvaal-A	1880 Ma	8° N	338° E	5°	6	Bates and Jones, 1996
Black Hills Dyke-Kaapvaal-B	1855 Ma	9° N	352° E	11.5°	6	Lubnina et al., 2010a
Kiuruvesi-Pielavesi-Fennoscandia-A	1886 Ma	41° N	231° E	5°	5	Neuvonen et al., 1981
Keuruu Dykes-Fennoscandia-B	1869 Ma	46° N	231° E	5.8°	7	Klein et al., 2016
Lower Atikan-Siberia	1878 Ma	31° N	279° E	5°	6	Didenko et al., 2009
Santa Rosa-Sobreiro Volcanics-Amazonia-A	1880 Ma	25° N	140° E	9.6°	7	Antonio et al., 2017
Velho-Guilherme Suite- Amazonia-B	1860 Ma	31° N	40° E	9	7	Antonio et al., 2017

Table 2. Paleomagnetic Poles used in Reconstructions-Continued

1770 Ma[5]						
Newer Dolerites- S. India	1765 Ma	45° N	311° E	8.7°	6	(see references table 1)
Mean Shoksa, Hotting,Lake Ladoga, Kallax Fennoscandia	1785 Ma	46° N	223°E	10°	6	Pisarevsky & Sokolov, 2001;Elming et al., 2009; Elming 1994, Mertanen et al., 2006
Volhyn-Dneister-Bug Sarmatia	1755 Ma	27° N	169° E	4°	7	Elming et al., 2010
Cleaver Dykes Laurentia	1741 Ma	19° N	277° E	6°	6	Irving et al., 2004
Avanavero mafic rocks Amazonia	1789 Ma	48° N	208° E	9°	6	Bispos-Santos et al., 2014
TH-ZR Dykes North China	1780 Ma	41° N	246° E	4°	7	Halls et al., 2000; Xu et al., 2014
Elgety Fm- Aldan Shield	1732 Ma	7° N	184° E	12.8°	7	Didenko et al., 2015
1450 Ma[6]						
Lakhna Dykes- S. India	1465 Ma	36° N	132° E	15.5°	5	Pisarevsky et al., 2014
Lake Ladoga Mafic Intrusions- Baltica	1457 Ma	12° N	173° E	7°	6	Lubinina et al., 2010b
St. Francois, Michikamau,Spokane, Tobacco Root, Purcell, Rocky Mountain-Laurentia	1450 Ma	11° N	37° E	10.7°	6	Meert and Stuckey, 2001; Elston et al., 2002; Emslie et al., 1976; Harlan et al., 2008; Elming and Pesonen, 2010
W. Anabar, N. Anabar, Sololi-Kyutinge-Siberia	1485 Ma	28° N	250° E	13.3°	5	Evans et al., 2016; Wingate et al., 2009
Curaçá- Congo-Sao Francisco	1507 Ma	10° N	10° E	15.8°	5	Salminen et al., 2016
Nova Guarita dykes-Amazonia	1419 Ma	48° N	66° E	6.5°	5	Bispos-Santos et al., 2012
Blue Range and Pandurra-S. Australia	1440 Ma	38° N	242° E	3.1°	4	Schmidt and Williams, 2011
Tieling Dykes- N. China	1437 Ma	12° N	187° E	5°	6	Wu, 2005

Rotation parameters for the reconstructions (-clockwise, +counterclockwise): [1]S India 0° N, 332° E, +77.2°; Yilgarn-A 0° N, 249.2° E, -100.2°; Yilgarn-B 0° N, 60° E, +67.3°; Kaapvaal 24.9° N, 42.9° E, +107.7°: [2]S. India 42.9° N, 64° E, 80.6°; Kaapvaal 22.3° N, 55° E, -168.4°; Slave-A 26.1° N, 210°E, -43.7°; Slave-B 51.3° N, 180° E, -104°; Superior 0° N, 10°E, -106°: [3] S. India 0° N, 94° E, +49.2°; Fennoscandia 0° N, 210.8° E, +65.3°; Superior 71.9° N, 176.9° E, +172.3°; Kaapvaal-A 26.7° N, 336.3° E, +61.2°; Kaapvaal-B 25.7° N, 320.8° E, +80.1°; Guiana Shield 0° N, 202.5° E, +88.2°;Greenland 19.3° N, 199° E, +78.1°: [4]S. India 0° N, 244° E, +55.9°;Fennoscandia-A 47.6° N, 171.3° E, +76°; Fennoscandia-B 50.8° N, 170.9° E, +73.3°; Kaapvaal-A 39° N, 293° E, +115.5°; Kaapvaal-B 40.1° N, 307° E, +114.4°; Slave 45° N, 90.5° E, +157.8°; Superior-A 47.4° N, 168° E, +97.4°;Superior-B 0° N, 155.8° E, +89° Amazonia-A 24.3° N, 5° E, -135.3°; Amazonia-B 29.5° N, 220.1° E, +180°; Siberia 28° N, 118.7° E, -160.5°; Wyoming 69.9° N, 307° E, -151.9°:[5]South India 20.3°N, 103.5° E, +159.7°; Fennoscandia 16.8° N, 140° E, +46.2°; Sarmatia 26.2° N, 26.6° E, -142.6°; Laurentia 0° N, 187° E, +71°; Amazonia 67.8° N, 188° E, +142.7°; North China 25.7° N, 168.8° E, -+54.1°;Aldan 33° N, 128.5° E, +104.2°:[6] S. India 26.9° N, 207° E, -61.2°; Laurentia 15.7° N, 287° E, -106.6°; Siberia 28.6° N, 45° E, 154.9°; Sao Francisco 22.6° N, 129.3° E, 111.7°; Amazonia 16.4° N, 286.5° E, -153°; S. Australia 25.2° N, 77° E, -167°; N. China 16.1° N, 263.5° E, -81.8°.